Chapter 5
Meteoric ^{7}Be and ^{10}Be as Process Tracers in the Environment

James M. Kaste and Mark Baskaran

Abstract ^{7}Be ($T_{1/2} = 53$ days) and ^{10}Be ($T_{1/2} = 1.4$ Ma) form via natural cosmogenic reactions in the atmosphere and are delivered to Earth's surface by wet and dry deposition. The distinct source term and near-constant fallout of these radionuclides onto soils, vegetation, waters, ice, and sediments makes them valuable tracers of a wide range of environmental processes operating over timescales from weeks to millions of years. Beryllium tends to form strong bonds with oxygen atoms, so ^{7}Be and ^{10}Be adsorb rapidly to organic and inorganic solid phases in the terrestrial and marine environment. Thus, cosmogenic isotopes of beryllium can be used to quantify surface age, sediment source, mixing rates, and particle residence and transit times in soils, streams, lakes, and the oceans. A number of caveats exist, however, for the general application of these radionuclides as tracers in the environment, as steady deposition and geochemical immobility are not guaranteed in all systems. Here we synthesize and review scientific literature documenting the deposition and behavior of these nuclides at the Earth's surface, focusing on current and potential applications for Earth scientists working to quantify terrestrial and marine processes.

5.1 Introduction

Cosmogenic isotopes of beryllium (Be) form when neutrons and protons spallate oxygen and nitrogen atoms (Fig. 5.1; Lal et al. 1958). The two naturally occurring Be isotopes of use to Earth scientists are the short-lived ^{7}Be ($T_{1/2} = 53.1$ days) and the longer-lived ^{10}Be ($T_{1/2} = 1.4$ Ma; Nishiizumi et al. 2007). Because cosmic rays that cause the initial cascade of neutrons and protons in the upper atmosphere responsible for the spallation reactions are attenuated by the mass of the atmosphere itself, production rates of comsogenic Be are three orders of magnitude higher in the stratosphere than they are at sea-level (Masarik and Beer 1999, 2009). Most of the production of cosmogenic Be therefore occurs in the upper atmosphere (5–30 km), although there is trace, but measurable production as oxygen atoms in minerals at the Earth's surface are spallated (in situ produced; see Lal 2011, Chap. 24). After cosmogenic Be is formed in the atmosphere, it is removed by rain, snow, and dry deposition. The near-constant production rate of cosmogenic Be isotopes in the atmosphere (Leya et al. 2000; Vonmoos et al. 2006) and the particle-reactive nature of the Be atom (You et al. 1989) make *meteoric* cosmogenic Be nuclides (sometimes referred to as "garden variety" to differentiate from in situ) a valuable tracer of a wide range of chemical, physical, and biogeochemical processes. Here we focus on the current and potential applications of meteoric ^{7}Be and ^{10}Be for quantifying and tracing natural processes occurring in soil, fluvial, lacustrian, and marine environments.

J.M. Kaste (✉)
Department of Geology, The College of William & Mary, Williamsburg, VA 23187, USA
e-mail: jmkaste@wm.edu
M. Baskaran
Department of Geology, Wayne State University, Detroit, MI 48202, USA
e-mail: Baskaran@wayne.edu

5.1.1 Production and Deposition of Meteoric ^{7}Be and ^{10}Be

The delivery of meteoric ^{7}Be and ^{10}Be to a particular point on the Earth's surface is controlled by the nuclide production rate in the atmosphere, the region's air mass source, amounts of precipitation, and the

M. Baskaran (ed.), *Handbook of Environmental Isotope Geochemistry*, Advances in Isotope Geochemistry,
DOI 10.1007/978-3-642-10637-8_5,

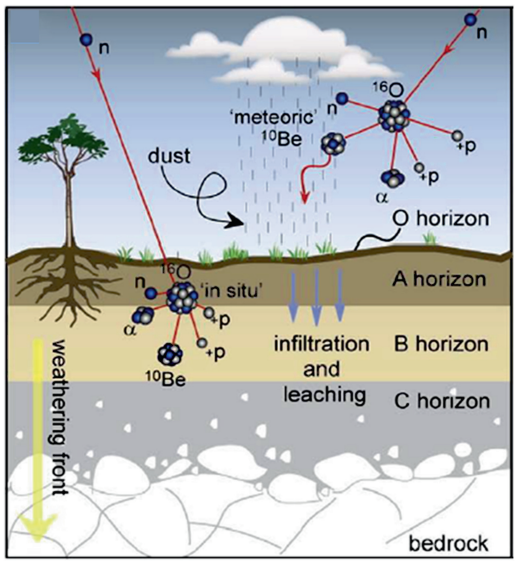

Fig. 5.1 Schematic of cosmogenic ^{10}Be production (^{7}Be forms in a similar manner). Meteoric ^{7}Be and ^{10}Be form in the atmosphere, and are delivered to the Earth's surface by wet and dry deposition. Most cosmogenic ^{7}Be is found on vegetation surfaces and in the O horizon or uppermost 2-cm of soil. Because of its longer half-life, ^{10}Be is commonly found on the surface, throughout the soil profile, and occasionally in saprolite. Reprinted from Willenbring and von Blanckenburg (2010a), Copyright (2010), with permission from Elsevier

efficiency of wet and dry depositional processes. Production rates of cosmogenic Be vary inversely with solar activity, because increased solar output strengthens the Earth's magnetic field which deflects cosmic rays. On timescales of decades, production rates vary by approximately 25% with the 11 year solar cycle, but over the course of hundreds of years, production rates may vary by a factor of two or more due to longer timescale modulations in the activity of the sun (Koch and Mann 1996; Vonmoos et al. 2006; Berggren et al. 2009). Because cosmic rays are deflected towards the poles, production rates of cosmogenic Be are a factor of 3–5 higher in polar air than in equatorial air (Harvey and Matthews 1989; Masarik and Beer 1999), depending on altitude. Polar air masses therefore have higher amounts of cosmogenic Be available for scavenging, but precipitation rates are generally very low here, which ultimately limits the meteoric radionuclide fluxes to the Earth's surface at high latitudes. The strong production gradient of cosmogenic Be with elevation in the atmosphere causes seasonal variability (at least in some latitude belts) in ^{7}Be and ^{10}Be deposition. This has been evident at mid-latitudes, as injections of stratospheric air into the troposphere during the spring season of each year result in higher concentrations of cosmogenic Be in meteoric waters (Husain et al. 1977). Stronger convection in the troposphere during summer months also increases ^{7}Be and ^{10}Be in rainfall as higher air is tapped (Baskaran 1995). Typically, fluxes of meteoric ^{7}Be and ^{10}Be to the Earth's surface scale with precipitation rates more than with latitude, and dry deposition generally is of lesser importance (Olsen et al. 1985; Brown et al. 1989; Wallbrink and Murray 1994; Whiting et al. 2005; Zhu and Olsen 2009), particularly for the shorter-lived ^{7}Be.

While the concentrations of cosmogenic Be in precipitation can vary by a factor of 20 between different storm events at one location, and are strongly dependent on latitude, amounts in rain and snow for each nuclide are commonly on the order of 10^{4} atoms g^{-1}, with ^{7}Be/^{10}Be atomic ratios falling between 0.41 and 0.61 in the Southern hemisphere and 0.67 and 0.85 in the Northern hemisphere (Brown et al. 1989; Knies et al. 1994). The production ratio of ^{7}Be/^{10}Be in the atmosphere is projected to be 1.9 (Nishiizumi et al. 1996; Masarik and Beer 1999); ^{7}Be/^{10}Be ratios measured in precipitation will be controlled by residence time in the atmosphere as ^{7}Be decays during air mass or aerosol transport. Snow commonly has higher concentrations of cosmogenic Be isotopes than rain, possibly because of the higher surface area of snowflakes compared with rain droplets (McNeary and Baskaran 2003). Concentrations of cosmogenic Be in precipitation compared from storm to storm are usually inversely proportional to rainfall amount, as aerosols are scavenged during the initial stages of a storm event and larger storms are simply more diluted (Olsen et al. 1985; Todd et al. 1989; Baskaran et al. 1993). For example, Ishikawa et al. (1995) documented a sharp reduction in the concentration of ^{7}Be in precipitation measured over the course of 2-day storm in Japan. During the first ~6 h of the storm, the ^{7}Be content of snowfall was approximately $10^{4.4}$ atoms g^{-1} (4 Bq L^{-1}), but this dropped to $<10^{3.8}$ atoms g^{-1} ($<$1 Bq L^{-1}) during the latter stages of the event. Resuspended dust can be a significant source of ^{10}Be in rain (Monaghan et al. 1986; Graham et al. 2003; Lal and Baskaran 2011), but is probably a minor source of ^{7}Be to meteoric waters because of its shorter half-life. The ^{10}Be content of continental dust is near that of the average concentrations in regional surface soil, which

indicates that topsoil erosion is the likely source of dust over continents (Gu et al. 1996). Lal (2007) estimated the global average value of atmospheric dust to be 2.12(±0.04) × 10^{9} ^{10}Be atoms g^{-1} dust.

It is presumed that once ^{7}Be or ^{10}Be is produced, it combines with atmospheric oxygen or hydroxyl to form Be oxide (BeO) or hydroxide ($BeOH_x^{2-x}$), molecules that are scavenged by atmospheric moisture. Equilibrium thermodynamics can be used to predict that in slightly acidic cloudwater or rainfall (pH <6), Be speciation will be dominated by Be^{2+} (Vesely et al. 1989; Takahashi et al. 1999). After rainfall hits the surface of the Earth, precipitation having a pH of <6 is usually neutralized rapidly, and cosmogenic Be quickly adsorbs to vegetation and the uppermost layer of soils and sediments (Pavich et al. 1984; Wallbrink and Murray 1996; Kaste et al. 2007). Because of the wide variability in the concentrations of cosmogenic Be isotopes in rainfall within storms, between storms, between seasons, and from year to year, and the potential of dust deposition being significant particularly for ^{10}Be, it takes several years worth of input measurements to accurately generalize deposition rates for a single location (Brown et al. 1989; Baskaran 1995). Furthermore, care must be taken to acidify samples because Be^{2+} can adsorb to plastic sampling funnels or collection bottles (Baskaran et al. 1993). A summary of the volume-weighted ^{7}Be concentrations measured in rainfall and calculated wet deposition fluxes is given in Table 5.1.

5.1.2 General Abundances of ^{7}Be and ^{10}Be at the Earth's Surface

Inventories of meteoric cosmogenic Be on the Earth's surface (in units of atoms (n) m^{-2} or activity (Bq = nλ) m^{-2}) at a particular location are a function of atmospheric deposition rates, exposure age, and soluble (from leaching or "desorption") and particulate (from erosion or sediment deposition) losses or gains. Soluble losses of cosmogenic Be from soils are thought to be negligible in watersheds of near-neutral pH, but can be appreciable in acidic systems (Pavich et al. 1985; Brown et al. 1992b). In most soils on gentle slopes, erosional losses of ^{7}Be are minimal because of its short half-life compared to the residence time of particle-reactive radionuclides in watersheds (or the timescale needed for significant erosion), but ^{10}Be inventory deficiencies are used to calculate steady-state erosion rates (Brown et al. 1995). ^{7}Be in soils may thus be in an approximate radioactive equilibrium with atmospheric deposition, such that decay rates roughly equal deposition rates on a Bq m^{-2} basis (Olsen et al. 1985). However, in areas where there is very strong seasonal variations of precipitation (such as San Francisco, CA and other areas controlled by seasonal monsoons such as East Asia, Southeast Asia, etc.), very high precipitation during certain months may result in transient equilibrium with much higher inventories in soils during wetter periods (Walling et al. 2009).

Generally, concentrations of ^{7}Be and ^{10}Be in soils and sediments near the Earth's surface are in the range of 10^{3}–10^{5} atoms g^{-1} (0.15–15 Bq kg^{-1}), and 10^{7}–10^{9} atoms g^{-1}, respectively (Fig. 5.2). Because of its short half-life, ^{7}Be is confined to vegetation and just the upper few cm of regolith and typically has an exponential decrease of concentration with depth in soils (Wallbrink and Murray 1996; Blake et al. 1999; Whiting et al. 2001; Wilson et al. 2003; Kaste et al. 2007). However, it may be found deeper than 10 cm in sedimentary environments with high deposition rates or where sediment mixing by bioturbation and/or physical mixing is significant (Canuel et al. 1990) or when there are flood events (Sommerfield et al. 1999). Vegetation plays a significant role in scavenging radionuclides from the atmosphere (Russell et al. 1981). A large fraction of the ^{7}Be surface inventory can reside in grasses or the forest canopy (Monaghan et al. 1983; Wallbrink and Murray 1996; Kaste et al. 2002) and decays before it can reach the top of the soil profile or enter into the hydrologic cycle. Surface ^{7}Be inventories typically range between $10^{8.8}$ and $10^{9.8}$ atoms m^{-2} (100–1,000 Bq m^{-2}; Table 5.1) and show some scaling with precipitation patterns (Whiting et al. 2005). Salisbury and Cartwright (2005) took a creative approach in quantifying ^{7}Be deposition along a precipitation gradient by showing that sheep feces sampled on a transect from sea-level to approximately 1,000 m in North Whales had approximately a fivefold gradient in ^{7}Be concentrations. They projected that rainfall rates increased by a factor of approximately three to four along this transect, and because much of the ^{7}Be was deposited directly on vegetation that the sheep ate, fresh feces recorded the deposition signal. An advantage of this technique is that it averages some of the spatial

Table 5.1 Compilation of ^{7}Be fallout fluxes and terrestrial surface inventories

Location	Latitude	Period of collection (month year^{-1})	Annual precipitation (cm)[a]	Average monthly ^{7}Be flux (Bq m^{-2} month^{-1})[a]	Volume-weighted ^{7}Be activity (Bq L^{-1})[a]	References
Precipitation-based collectors						
Bombay (India)	29°0′N	1955–1961, 1963–1965, 1968, 1970	230	106	0.55	Lal et al. (1979)
Galveston, TX	29°18′N	12/1988–2/1992	117 (97–150)	204 (124–322)	1.45–2.58 (2.03)	Baskaran et al. (1993)
College Station, TX	30°35′N	6/1989–2/1992	122 (98–146)	192 (174–208)	1.73–2.07 (1.90)	Baskaran et al. (1993)
Bermuda	32°20′N	9/1977–8/1978	170	238	1.57	Turekian et al. (1983)
Oak Ridge, TN	35°58′N	9/1982–8/1984	127 (110–143)	169 (142–196)	1.60 (1.55–1.65)	Olsen et al. (1986)
Norfolk, VA	36°53′N	1/1983–12/1984	136 (132–141)	173 (167–179)	1.58 (1.50–1.67)	Todd et al. (1989)
Ansan, S. Korea	37°17′N	1/1992–6/1993	112 (106–117)	142	1.08	Kim et al. (1998)
Solomon, MD	38°19′N	3/1986–11/1987	96	189	2.36	Dibb and Rice (1989b)
Onagawa, Japan	38°26′N	4/1987–3/1989	115 (88–142)	150 (118–181)	1.57 (1.54–1.60)	Ishikawa et al. (1995)
Thessaloniki, Greece	40°38′N	1/1987–4/1990	48 (33–65)	51(40–70)	1.29 (1.10–1.48)	Papastefanou and Ioannidou (1991)
Westwood, NJ	40°59′N	12/1960–8/1961	78	60	0.92	Walton and Fried (1962)
New Haven, CT	41°31′N	3/1977–6/1978	148	315	2.63	Turekian et al. (1983)
Detroit, MI	42°25′N	9/1999–2/2001	76	181	2.87	McNeary and Baskaran (2003)
Geneva, Switzerland	46°16′N	11/1997–11/1998	97	174	2.16	Caillet et al. (2001)
Lake Geneva, Switzerland	46°30′N		120	230	2.30	Dominik et al. (1987)
Lake Zurich, Switzerland	47°22′N		110	223	2.43	Schuler et al. (1991)
Quillayute, Wash.	47°57′N	2/1976–1/1977	270	113	0.50	Crecelius (1981)
Chilton, England	51°26′N	10/1959–9/1960	68	76	1.35	Peirson (1963)
Milford, England	51°42′N	10/1959–9/1960	63	72	1.38	Peirson (1963)
Rijswijk, Netherlands	52°01′N	11/1960–10/1961	93	132	1.70	Bleichrodt and Van Abkoude (1963)
Terrestrial surface inventories						
		Collection date (month/year)	Median surface inventory (Bq m^{-2})	^{7}Be flux (Bq m^{-2} month^{-1})[b]	Surface type	
SE Queensland, AU	28°01′S	5/2003	440	175	Soil	Doering et al. (2006)
Black Mtn, Australia	35°15′S	9/1988	200	79	Soil + overlying grass	Wallbrink and Murray (1996)
Black Mtn, Australia	35°15′S	9/1988	130	52	Alluvial bare soil	Wallbrink and Murray (1996)
Black Mtn, Australia	35°15′S	5/1989	400	159	Soil + overlying grass	Wallbrink and Murray (1996)
Black Mtn, Australia	35°15′S	5/1989	155	61	Alluvial bare soil	Wallbrink and Murray (1996)
Oak Ridge, TN	35°58′N	7/1984	673	267	Soil + overlying grass	Olsen et al. (1985)
Owens Valley, CA	37°22′N	10/2006	85	34	Soil + grass	Elmore et al. (2008)
Wallops Island, VA	37°55′N	1/1985	673	267	Marsh + overlying grass	Olsen et al. (1985)
Wallops Island, VA	37°55′N	1/1985	107	42	Unvegetated marsh	Olsen et al. (1985)
Mendocino, CA	39°18′N	6/1980	700	278	Above-ground vegetation and litter	Monaghan et al. (1983)
Delaware Marsh	39°27′N	7/1982	207	82	Marsh + overlying grass	Olsen et al. (1985)
Valdivia, Chile	39°44′S	9/2003	573	227	Soil	Schuller et al. (2006)
Valdivia Chile	39°49′S	4/2006	522	207	Recently harvested forest soil	Walling et al. (2009)
Valdivia Chile	39°49′S	10/2006	1,139	452	Recently harvested forest soil	Walling et al. (2009)
Central Idaho	44°50′N	5/1996	139	55	Soil + overlying vegetation	Bonniwell et al. (1999)
Central Maine	44°50′N	12/98	554	220	Bog core + overlying vegetation	Kaste (1999)
Cooke City, MT	45°01′N	6/2000	449	178	Soil	Whiting et al. (2005)
Devon, UK	50°47′N	2/1998	512	203	Soil	Blake et al. (1999)

[a]Numbers in parenthesis denote the range when data are reported for ≥2 years

[b]Assumes steady-state between surface and atmospheric flux: calculated by multiplying the median surface inventory (Bq m^{-2}) by 0.3966 month^{-1}

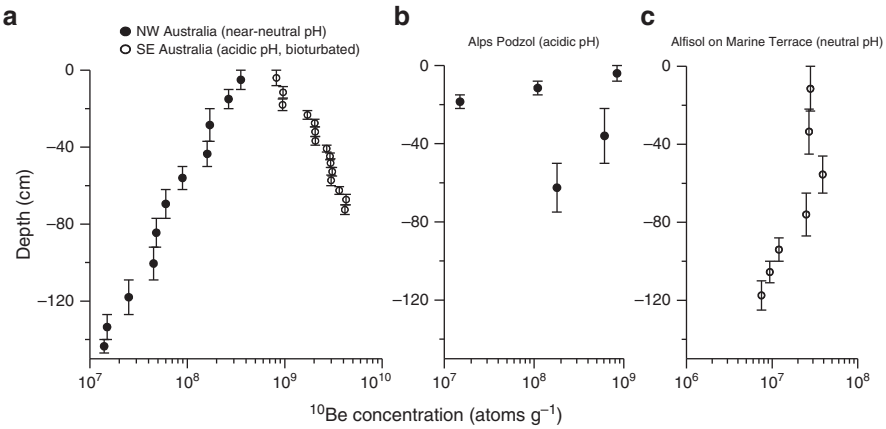

Fig. 5.2 Concentrations of meteoric ^{10}Be with depth in (**a**) a neutral pH soil profile in NW Australia and an acidic soil that was strongly bioturbated in SE Australia (Fifield et al. 2010), (**b**) an acidic Podzol from the Alps (Egli et al. 2010), and (**c**) a near-neutral pH soil developed on a marine terrace in California (Monaghan et al. 1992)

heterogeneity associated with atmospheric deposition on vegetated terrain. Because the half-life of ^{10}Be is ~8 orders of magnitude larger than the residence time of aerosols in the atmosphere, in temperate to tropical regions where the air is stripped of cosmogenic Be isotopes in the initial part of storms, ^{10}Be inventories may not be controlled by rainfall rate as higher rainfall amounts simply dilute concentrations but do not add to the flux (Willenbring and von Blanckenburg 2010a). The fact that small changes in amount of precipitation for a region may not significantly alter depositional fluxes makes it slightly simpler to project steady-state ^{10}Be inventories for a landform.

5.2 Background

5.2.1 General Geochemical Behavior of Be in the Environment

Beryllium has the smallest ionic radius (0.31 Å) of all the metal cations, and exists only in the +2 valence state in natural aqueous solutions (Baes and Mesmer 1976). Its first hydrolysis constant $\{[H^+][BeOH^+]/[Be^{2+}]\}$ is $10^{-5.7}$; hence in meteoric waters where pH is controlled by atmospheric CO_2, there should be a near equal distribution of the divalent cation $[Be^{2+}]$ and its first hydrolysis product $[BeOH^+]$. In acidic precipitation where anthropogenic acids have depressed the pH of rainfall to <5.5, much of the meteoric cosmogenic Be may exist as Be^{2+}, whereas in regions where rainfall pH is buffered by calcite-bearing dust, cosmogenic Be may be in the $BeOH^+$ form. Given the typical pH range of natural waters of 5–9, equilibrium-based thermodynamic models would predict that the relative Be species abundances and the partitioning of cosmogenic Be may vary by orders of magnitude between slightly acidic systems and more alkaline systems. Indeed, experimental studies demonstrate that the partitioning of Be from the aqueous phase to an adsorbed phase on a range of materials is strongly pH dependent (Bloom and Crecelius 1983; Hawley et al. 1986; You et al. 1989). Using 3-week equilibration periods, You et al. (1989) showed a >100-fold variation in the solid-phase partitioning coefficient (K_d in kg L^{-1}) over the pH range of 4–8 for different substrate types (Fig. 5.3).

In freshwater rivers, amounts of dissolved ^{7}Be in the water column are commonly below detection limits (Dominik et al. 1987; Bonniwell et al. 1999), but in marine environments, Be may be characterized as having a limited affinity for suspended matter, as large fraction of the ^{7}Be and ^{10}Be appears to be dissolved (Merrill et al. 1960; Bloom and Crecelius 1983; Kusakabe et al. 1987; Dibb and Rice 1989a; Measures et al. 1996). The mechanism of Be adsorption onto inorganic minerals, including primary silicate minerals, secondary silicates, and iron and aluminum oxyhydroxides is typically considered to be via the formation of a complex between the Be atom and oxygen on

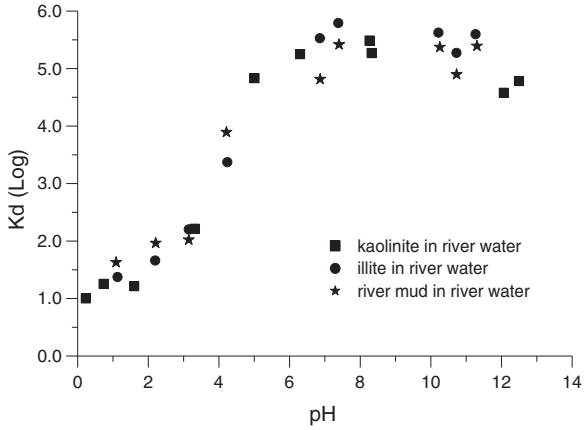

Fig. 5.3 The dependence of the K_D of Be for different materials over varying pH, using equilibration times of 3 weeks and suspended solids concentrations of 0.2 g L^{-1}. Reprinted from You et al. (1989), Copyright (1989), with permission from Elsevier

the surfaces or corners of minerals ("inner sphere adsorption"). The K_d may increase on timescales of weeks to months as adsorption-desorption equilibrium is followed by cationic lattice substitution (Nyffeler et al. 1984; Dibb and Rice 1989a). Like other particle-reactive metals, the K_d varies inversely with suspended solids concentrations below 30 mg L^{-1} (Hawley et al. 1986). While Be can form complexes with organic matter functional groups (daSilva et al. 1996), its partitioning coefficients seem to be significantly higher for inorganic materials compared with algae or seston (Bloom and Crecelius 1983; Dibb and Rice 1989a). Selective chemical extractions of marine sediments (Bourles et al. 1989) and soils (Barg et al. 1997) show that most of the meteoric Be is associated with authigenic phases (secondary Al, Fe, and Mn minerals) and organic matter coatings. Beryllium forms strong complexes with fluoride and humate, which could theoretically affect the strength and rate of aqueous to solid-phase partitioning (Nyffeler et al. 1984; Vesely et al. 1989; Takahashi et al. 1999).

The depth to which meteoric Be penetrates in soils and sediments will be controlled by advection (leaching or percolation) and diffusion-like (mixing) processes. The short half-life and tendency to adsorb to the solid phase causes ^{7}Be to generally be fixed in the vegetation and upper 2-cm of soil (Wallbrink and Murray 1996; Walling et al. 2009), but meteoric ^{10}Be is usually detectable from the soil surface to the C horizon, and in some cases through saprolite (Pavich et al. 1985). In high pH soils that are not intensively mixed, fallout Be exhibit an exponential decline in concentrations with depth (Fig. 5.2a, NW Australia Site) as the affinity of the Be atom for the surface of almost any material (layered clays, secondary oxide minerals, organic matter, etc.) will be very strong. In acidic soil profiles, however, the Be atom may be highly enriched in specific layers that have the most favorable surface sites for adsorption (Fig. 5.2a, b). In most near-neutral pH soils, the concentration of meteoric ^{10}Be in soils has a subsurface concentration maximum in the B horizon layer where iron and aluminum accumulate (Barg et al. 1997; Jungers et al. 2009; Egli et al. 2010); beneath this there is often a general exponential decrease with depth (Fig. 5.2c). Physical soil mixing by organisms, wetting-drying cycles, or freeze-thaw cycles appears to create a layer of homogenized ^{10}Be concentrations (Fifield et al. 2010) as seen in the SE Australia ^{10}Be profile given in Fig. 5.2a.

5.2.1.1 Cosmogenic ^{7}Be and ^{10}Be in Freshwater Environments

The few watershed-scale studies that measure ^{7}Be and/or ^{10}Be in soils and waters have demonstrated that the actual distribution of Be between the solid and aqueous phase is broadly consistent with the thermodynamic predictions described above. In a survey of tropical watersheds in the Orinoco and Amazon basin, Brown et al. (1992b) found that acidic drainage waters had nearly the same concentration of dissolved ^{10}Be as incoming precipitation, indicating very little adsorption to soils and sediments. In more neutral to alkaline waters, concentrations of dissolved ^{10}Be in streamwater are often orders of magnitude smaller than meteoric waters because of adsorption to aluminum and iron oxide coatings on soils and sediments (Brown et al. 1992b; Barg et al. 1997) (Fig. 5.3).

Because of its shorter half-life and tendency to adsorb, the vast majority of ^{7}Be is retained by the vegetation and upper soils of a watershed (Olsen et al. 1986; Cooper et al. 1991; Wallbrink and Murray 1996; Bonniwell et al. 1999). Even during snowmelt events when the storm hydrograph is dominated by new water, most ^{7}Be never reaches the stream (Cooper et al. 1991). There are no reports of ^{7}Be in groundwater above typical detection limits ($<$10 atoms g^{-1} or 1.5 mBq L^{-1}). Due to the short half-life and high K_ds of ^{7}Be, it is not expected to penetrate very far beyond soil-air interface and hence it is not expected to be present in groundwater. In freshwater rivers,

concentrations of dissolved (<0.45 μm) ^{7}Be are usually on the order of undetectable to 10^{2} atoms g^{-1} (15 mBq L^{-1}), which is orders of magnitude lower than levels usually found in precipitation. Suspended sediments in streams however can have ^{7}Be concentrations on the order of 10^{6} atoms g^{-1} (100–200 Bq kg^{-1}) (Dominik et al. 1987; Bonniwell et al. 1999); export of ^{7}Be from watersheds is evidently dominated by erosion and particulate losses. The concentration of dissolved ^{7}Be in lakes can vary by an order of magnitude over the course of a year as biological productivity varies with seasons. A sub-alpine lake in Bodensee had dissolved concentrations of ^{7}Be fluctuating from approximately $10^{0.8}$–$10^{1.8}$ atoms g^{-1} (1–10 mBq L^{-1}) over the course of the year, which appeared to be controlled by the availability of particulates that are ultimately regulated by biological processes (Vogler et al. 1996).

Cosmogenic ^{10}Be in groundwater has been reported to range from 10^{2} to 10^{3} atoms g^{-1} (Pavich et al. 1985; McHargue and Damon 1991). Pavich et al. (1985) calculated that the groundwater losses of ^{10}Be from a watershed in Virginia were three orders of magnitude lower than meteoric inputs. In a general survey of North American rivers and the Pearl River Basin in China, Kusakabe et al. (1991) reported dissolved concentrations of ^{10}Be to range from approximately 10^{3}–$10^{3.7}$ atoms g^{-1}, which was slightly less than the ^{10}Be content of rainfall, but an order of magnitude higher than the amounts found in estuaries. However, dissolved ^{10}Be in the slightly acidic Orinoco River was found to be nearly equivalent to concentrations measured in local precipitation (Brown et al. 1992b). It seems that in acidic watersheds, the exchange sites on mineral surfaces may be dominated by other ions (H^{+}, Al, etc.), which may inhibit Be adsorption. McHargue and Damon (1991) used an average ^{10}Be concentration of 10^{3} atoms g^{-1} for freshwaters, the volume of water in the world's rivers and lakes, and the global annual runoff flux to calculate that the residence time of ^{10}Be in the world's freshwaters is approximately 3 years.

5.2.1.2 Cosmogenic ^{7}Be and ^{10}Be in the Marine Environments

After Be radionuclides are delivered to the air-water interface via wet and dry fallout, the ions are removed from the water column primarily by adsorption onto particulate matter. While the removal rate is strongly dependent on the concentration and composition of suspended particulate matter (Dibb and Rice 1989a), the residence time of dissolved Be above the thermocline is on the order of 0.5 years (Fig. 5.4), which

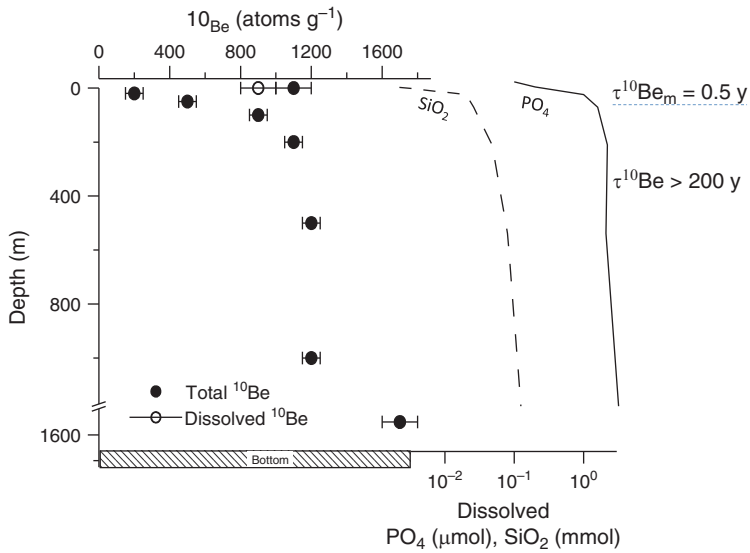

Fig. 5.4 ^{10}Be, phosphate, and silica concentrations in the water column in the San Nicolas Basin (Kusakabe et al. 1982). Above the thermocline in the "mixed layer" (upper ~100 m), high concentrations of suspended particles cause rapid removal of dissolved Be from the water column. As the particles dissolve beneath the thermocline, ^{10}Be is recycled back into the water column where it has a residence time of hundreds of years

is similar to the residence times reported for other particle-reactive atoms like Th and Pb (Kusakabe et al. 1982). The first measurement of ^{7}Be in seawater from the Indian Ocean was reported by Lal et al. (1960). Silker et al. (1968) later demonstrated that ^{7}Be had relatively uniform dissolved concentrations in surface waters of the Atlantic Ocean (5°48′–25°38′N, $n = 7$ samples), ranging from $10^{1.4}$ to $10^{1.7}$ atoms ^{7}Be g^{-1} (40–70 mBq L^{-1}), with a particulate fraction ranging between 7.4 and 14.9% of the total. Kusakabe et al. (1982) found that concentrations of ^{10}Be measured in unfiltered water samples collected from the surface of San Nicolas Basin were indistinguishable from the ^{10}Be measured in filtered water samples (Nucleopore 0.4 μm filter), and concluded that most ^{10}Be was in dissolved form (Fig. 5.4).

Although the monthly depositional fluxes of ^{7}Be have been reported to vary by a factor of ~10, in the water column of the ocean, activities (Bq L^{-1}) vary much less, as the water column integrates the activities over its mean life. The amount of precipitation on the ocean varies with latitude and season, which will affect the depositional fluxes of ^{7}Be and thus their water column inventories. Concentrations of particulate and dissolved ^{7}Be within an estuarine system vary spatially and temporally. For example, the particulate and total (total = dissolved + particulate) ^{7}Be activities in June 2003 in Tampa Bay, Florida varied between $10^{-0.5}$ and $10^{0.4}$ atoms g^{-1} (0.05 and 0.39 mBq L^{-1}) and 10 and $10^{2.5}$ atoms g^{-1} (1.7 and 49 mBq L^{-1}), respectively while the corresponding values varied between $10^{0.3}$ and $10^{1.4}$ atoms g^{-1} (0.3 and 3.7 mBq L^{-1}) and $10^{1.1}$ and $10^{2.3}$ atoms g^{-1} (2 and 28 mBq L^{-1}), respectively in August 2003 (Baskaran and Swarzenski 2007). Particulate ^{7}Be concentrations are generally higher in the spring compared with summer, mainly due to higher amounts of water discharge and precipitation in late spring and early summer months, which results in higher particulate fluxes, resuspension, and scavenging during that time. The total residence time of ^{7}Be (τ_{Be}) is calculated using a simple approach, assuming that the water column is uniformly-mixed:

$$\tau_{Be} = \ln 2 \times A_{Be} \times h/I_{Be} \quad (5.1)$$

where A_{Be} is the total activity of ^{7}Be (Bq m^{-3}), I_{Be} is the atmospheric input rate of ^{7}Be (Bq m^{-2} day^{-1}), and h is the mean depth (m) of the well-mixed sampling area. The residence time of dissolved Be in coastal waters varies over an order of magnitude, from <1 to 60 days, depending on the depth of the coastal/estuarine waters and concentrations of suspended particulate matter (Table 5.2). The K_d values in coastal waters may vary over two orders of magnitude, between 7×10^3 and 1.2×10^6 (Olsen et al. 1986; Baskaran and Santschi 1993; Baskaran et al. 1997; Kaste et al. 2002; Jweda et al. 2008). The K_d values are reported to be higher in June than in August, which is related to the variations in the amount of freshwater discharge and the amounts of precipitation that control the extent of resuspension of bottom sediments.

Table 5.2 Residence time of dissolved ^{7}Be in various coastal waters

Location	Residence time of ^{7}Be (d)	References
New York Harbor	8–17	Olsen et al. (1986)
James River Estuary	2–4	Olsen et al. (1986)
Raritan Bay	7–17	Olsen et al. (1986)
Chesapeake Bay	5–52	Dibb and Rice (1989a)
Galveston Bay	0.9–1.8	Baskaran and Santschi (1993)
Sabine-Neches estuary	0.8–10.5	Baskaran et al. (1997)
Tampa Bay	1.6–58.7	Baskaran and Swarzenski (2007)
Clinton River	1.0–60.3	Jweda et al. (2008)
Hudson River Estuary	0.7–9.5	Feng et al. (1999)

The concentration of dissolved ^{10}Be in marine surface waters typically varies between $10^{2.6}$ and $10^{3.2}$ atoms g^{-1}, and the residence time of Be has been generally reported to be shorter than the mixing time of the oceans (Merrill et al. 1960; Frank et al. 2009). Meltwaters from glaciers (both polar and high-altitude) could have higher concentrations of ^{10}Be compared with surrounding waters (e.g., Antarctic ice contains about $10^{4.7}$ atom g^{-1} of ^{10}Be, Raisbeck et al. 1978b). With the exception of one dataset, all data indicate that the water column inventory of ^{10}Be, in the Pacific is higher than that in the Atlantic (Table 5.3), perhaps a result of lower suspended matter concentrations in the Pacific. The transfer of ^{10}Be from the dissolved phase to the solid (adsorbed) phase may be regulated by the recycling of biogenic particles in the oceans (Fig. 5.4).

A wide range of dissolved residence times of ^{10}Be in the open ocean have been reported in the literature. Several approaches have been used to obtain residence times that include the inventories of ^{10}Be and annual

removal or depositional input of ^{10}Be, and from the Fe-Mn crust and Mn-nodule measurements (Raisbeck et al. 1978a, 1980; Kusakabe et al. 1982, 1987; Segl et al. 1987; Anderson et al. 1990; Ku et al. 1990; Brown et al. 1992a; Measures et al. 1996; von Blanckenburg et al. 1996; Frank et al. 2002, 2009). A large range of residence time values, if real, has major implications on the changing geochemical processes that lead to varying removal rates of Be^{2+} from the water column. In order to assess the variations, the data from all the open ocean sites were recalculated to determine the inventories of ^{10}Be in the water column (a standard depth of 3,600 m was used for all the basins) and the inventories are given in Table 5.3. Except the Arctic Ocean, where we compared the residence times of ^{10}Be in all four major basins (Nansen, Amundsen, Makarov and Canada Basins), we used the same depositional flux for each of the sites. The vertical profiles of dissolved ^{10}Be from these four basins are given in Fig. 5.5. The errors associated with the concentrations of ^{10}Be in individual depths reported in the publications are propagated to obtain the error associated with the inventory, which we use in the calculation of the errors associated with the residence times. The residence time of ^{10}Be in these major deep basins of the Arctic Ocean ranged from 680 to 830 years (Table 5.3), and given the propagated errors, there is no discernable difference in the residence time of ^{10}Be between the four basins of the Arctic. This observation can be compared to another particle-reactive radionuclide, Th in these major basins. A compilation of ^{230}Th data from these four basins clearly showed that the residence time of Th in the Makarov Basin is the longest (45 $\pm$ 1 years) compared to Canada Basin (22 $\pm$ 2 years), Amundsen Basin (19 $\pm$ 1 years) and Nansen Basin (17 $\pm$ 2 years; Trimble et al. 2004). The lack of difference we observe with ^{10}Be could be real or due to using the same atmospheric depositional input of 0.25×10^{6} atoms cm^{-2} year^{-1} (Frank et al. 2009) for all four basins. Since the annual removal rate and annual depositional flux data are sparse, we do not know whether there is a real difference between the residence times, but there are real differences between the particle concentrations and particle fluxes between these basins (Trimble et al. 2004).

Our calculated residence time given in Table 5.3 varies by a factor of 2.4 (between 236 and 505 years) between the Atlantic (western North Atlantic, South Atlantic) and Pacific Ocean. Thus, it appears that the

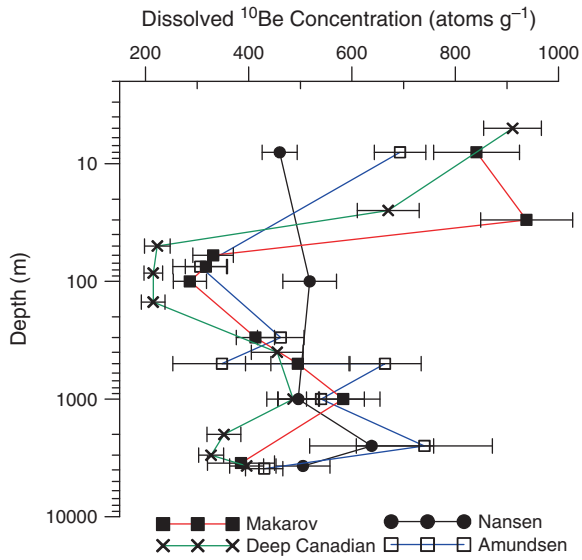

Fig. 5.5 Vertical profiles of dissolved ^{10}Be concentrations from all four major deep basins of the Arctic Ocean. Data are plotted from Frank et al. (2009)

wider range of residence times reported by various authors in the past (factor of ~10) may be due to poorly constrained input term used in their calculations. Lao et al. (1992a) estimated the deposition rate of ^{10}Be for the entire Pacific Ocean to be 1.5×10^{6} atoms cm^{-2} year^{-1}, during the Holocene based on dated sediment cores. While the inventories can be measured precisely (with better than 10% precision), the annual depositional (input) flux is more difficult to constrain, as it can significantly vary depending on the amount of precipitation. Multi-year depositional flux measurement could reduce the uncertainty in the depositional flux. Perhaps by quantifying the relationship between ^{10}Be and another fallout isotope that is easier to measure in rainfall or has longer term datasets available (e.g., ^{210}Pb, Preiss et al. 1996; Sheets and Lawrence 1999), the depositional fluxes of ^{10}Be could be better constrained for residence time calculations.

5.2.2 Measuring ^{7}Be and ^{10}Be in Environmental Samples

5.2.2.1 Preconcentration Methods

The concentrations of ^{7}Be in surface water samples are so dilute a preconcentration method is usually needed.

Table 5.3 Concentrations, inventories and residences times of dissolved ^{10}Be in the major world oceans

Sample code	Coordinates	Depth (m)	Surface water ^{10}Be (atoms g^{-1})	^{10}Be inventory (10^8 atoms cm^{-2})	Residence time (years)	References
Arctic ocean						
Nansen Basin	84°16.87′N; 33°39.81′E	4,039	460	1.98 ± 0.30	790 ± 120	Frank et al. (2009)[1]
Amundsen Basin	88°24.48′N; 95°22.78′E	4,400	693	2.08 ± 0.38	830 ± 150	Frank et al. (2009)[1]
Makarov Basin	87°54.97′N; 154°22.50′E	3,985	841	1.70 ± 0.15	680 ± 60	Frank et al. (2009)[1]
Canada Basin	75°12.5′N; 149°57.0′W	3,850	911	1.72 ± 0.24	690 ± 96	Frank et al. (2009)[1]
Atlantic ocean						
Transect at 25°N	25°N; 60°W	>4,500	1,407	4.50 ± 0.22	372 ± 18	Segl et al. (1987)[2]
Transect at 25°N	26°N; 50°W	>4,500	1,671	6.80 ± 0.78	562 ± 64	Segl et al. (1987)[2]
Transect at 25°N	27°N; 44–45°W	>3,319	1,310	5.98 ± 0.70	494 ± 58	Segl et al. (1987)[2]
Transect at 25°N	27°N; 35°W	>4,500	1,416	4.57 ± 0.59	378 ± 49	Segl et al. (1987)[2]
Western North A.	41°32′N; 63°37′W	>3,411	430	2.85 ± 0.18	236 ± 15	Ku et al. (1990)[3]
Western North A.	34°1′N; 63°0′W	>5,178	640	2.94 ± 0.22	243 ± 18	Ku et al. (1990)[3]
South Atlantic	24°40′S; 38°21′W	>3,830	930	3.35 ± 0.14	279 ± 12	Measures et al. (1990)[4]
South Atlantic	24°55′S; 01°00′W	>4,152	585	3.66 ± 0.16	305 ± 13	Measures et al. (1990)[4]
South Atlantic	01°59′S; 04°02′W	>4,850	671	3.12 ± 0.13	260 ± 13	Measures et al. (1990)[4]
Drake Passage	57–63°S; 66–69°′W	>3,700	1,400	4.97 ± 0.41	49 ± 12[a] (279 ± 12)[a]	Kusakabe et al. (1982)
Pacific Ocean	25°00′N; 169°59′E	6,013	1,060	5.74 ± 0.36	879 ± 54[b] (475 ± 29)[b]	Kusakabe et al. (1987)
Pacific Ocean	17°28′N; 117°58′W	3,950	610	5.74 ± 0.33	870 ± 50[b] (475 ± 27)[b]	Kusakabe et al. (1987)
Pacific Ocean	2°46′S; 117°02′W	4,200	810	6.11 ± 0.27	926 ± 41[b] (505 ± 22)[b]	Kusakabe et al. (1987)

The following atmospheric inputs were assumed: 1: 2.5×10^5 atoms cm^{-2} year^{-1} (Frank et al. 2009); 2: 1.21×10^6 atoms cm^{-2} year^{-1} (Segl et al. 1987); 3: 1.21×10^6 atoms cm^{-2} year^{-1} (Monaghan et al. 1986); 4: 1.21×10^6 atoms cm^{-2} year^{-1} was assumed

[a]Downward flux of 6.9×10^6 atoms cm^{-2} year^{-1} calculated using concentration gradient in ^{10}Be and assuming a vertical diffusivity (Kusakabe et al. 1982); the number in parenthesis is calculated assuming 1.21×10^6 atoms cm^{-2} year^{-1} (Monaghan et al. 1986)

[b]Influx value of 6.6×10^5 atoms cm^{-2} year^{-1} was assumed (Kusakabe et al. 1987); the number in parenthesis is calculated assuming 1.21×10^6 atoms cm^{-2} year^{-1} (Monaghan et al. 1986)

This is particularly important for partitioning studies in lakes, rivers and marine system which require precise measurements in the particulate and dissolved phases. For the extraction of particulate matter, filter cartridges have been widely employed (Silker 1972; Baskaran et al. 1997, 2009b; Feng et al. 1999; Baskaran and Swarzenski 2007). When the dissolved phase (<pore-size of the filter, either absolute cut-off or nominal) is passed through a prefilter, it is possible that some of the dissolved phase may sorb onto the polypropylene/acrylic/glass filters. So far, no studies have been made to quantify this, although recent work indicates that a finite fraction of the dissolved Th is removed by the prefilter (Baskaran et al. 2009b). For preconcentrating the dissolved phase, three common methods are employed that include: (1) evaporation; (2) co-precipitation; and (3) ion-extraction or extraction onto sorbents. Of these three methods, very low ionic strength solutions, including rainwater and freshwaters can be evaporated to reduce the volume (as low as 5–10 mL) that can be directly gamma-counted in Ge-well detectors. Evaporation of seawater samples will result in large amount of salts (~35 g L^{-1} of seawater) and hence it is not the suitable method for seawaters and other waters with high total dissolved solids. Co-precipitation with $FeCl_3$ is one of the most

common methods employed to preconcentrate; detailed procedures are given in Baskaran et al. (2009b). Stable Be carrier is added as yield monitor. Sorbents that have been utilized to extract dissolved radionuclides include $Fe(OH)_3$-impregnated fibers and a bed of aluminum oxide (Lee et al. 1991; Kadko and Olson 1996). Silker (1972) demonstrated that a flow rate of 35 L min^{-1} through a 6.4 mm thick alumina bed removed 70% of the ^{7}Be from seawater. Kadko and Olson (1996) assumed a constant efficiency of $69 \pm 3\%$, although most cartridge methods for particle-reactive radionuclides (such as Th, Pb, etc.) have been found to have variable extraction efficiencies (Baskaran et al. 2009a). The constant efficiency assumption for Be removal needs to be rigorously tested. Concentrations of ^{10}Be in surface waters of the global ocean vary between 10^2 and 10^3 atoms g^{-1} (Raisbeck et al. 1978a; Kusakabe et al. 1982, 1990; Ku et al. 1990; Frank et al. 2009) and hence preconcentration is required. A minimum of a 2-L water sample (~0.4–2 $\times$ 10^7 atoms) is needed and details on chemical separation and purification are given in Baskaran et al. (2009b). For ^{10}Be analysis, sediments and aerosol samples are digested with concentrated HF, HNO_3, HCl and brought to solution with the addition of ^{9}Be carrier. Beryllium from this digested solution can be separated and purified following the procedure summarized in Baskaran et al. (2009b). The purified Be in the form of $Be(OH)_2$ is mixed with a small amount of $AgNO_3$ powder and then ashed at 850°C for 6 h and the ashed BeO powder is to prepare the target for the AMS analysis. Although the separation and purification of ^{10}Be is straight forward, isobaric interference from boron isotopes (^{10}B) could affect the measurements of ^{10}Be by AMS and hence care must be exercised in the purification of Be to eliminate B. Earlier studies added ^{7}Be spike (obtained from a commercial company) for the measurements of ^{10}Be in seawater as a yield monitor which had a high blank levels of ^{10}Be and hence caution needs to be exercised in utilizing ^{7}Be spike as a yield monitor (Kusakabe et al. 1982).

5.2.2.2 Measurement of ^{7}Be and ^{10}Be Concentrations

^{7}Be is most commonly measured in environmental samples using low-background decay counting techniques (Arnold and Al-Salih 1955; Larsen and Cutshall 1981). ^{7}Be decays to ^{7}Li via electron capture, with 89.6% of the decays emitting a very low energy x-ray as they go directly to the ground state, and 10.4% of the decays first going to an excited state, which is the fraction that emits the 477.6 keV gamma. Gamma measurements are usually done using shielded scintillation detectors (e.g., NaI crystals) or semiconductor detectors made of Ge(Li) or pure (intrinsic) germanium (Arnold and Al-Salih 1955; Silker 1972; Larsen and Cutshall 1981; Krishnaswami et al. 1982; Murray et al. 1987; Baskaran et al. 1997; Baskaran and Shaw 2001). The absolute detection efficiency of NaI detectors for gamma rays is typically higher than the efficiency of Ge detectors, but NaI detectors have poor energy resolution. The width of the peak at half of the maximum value (full width at half maximum, FWHM of the Gaussian curve) for NaI detectors at 478 keV is commonly $\geq$30 keV, which is inadequate for resolving the ^{7}Be gamma from possible emissions from U and Th series isotopes. Most notably, ^{228}Ac (^{232}Th series) has a strong emission (4.74% yield) at 463 keV (Dalmasso et al. 1987), and radon progeny have low yield emissions at 480 and 487 keV (Morel et al. 2004) which can be significant when counting samples high in ^{226}Ra. Separation and purification of the Be atom is therefore necessary when using scintillation detectors, but Ge(Li) and intrinsic Ge detectors have high enough resolution (~1–2 keV FWHM) in the 478 keV region which allows for the direct analysis of soils, sediments, waters, or filter papers for the ^{7}Be gamma.

One of the most important considerations that must be made when analyzing for ^{7}Be is the background of the gamma spectrum, which can control the detection limits. Compton scattering occurs when high energy gammas eject an electron with only a fraction of their full energy, which can create a "count" on the detector's spectrum and a newer lower energy gamma ray that can also create counts on the detector. Thus, high energy photons (>500 keV) from the U and Th decay series, ^{40}K, and cosmic rays thus generate random noise in the region of the gamma spectrum where ^{7}Be decays. By completely surrounding the scintillation or Ge detectors with 4″ of lead and using detector hardware (preamplifier, wires, etc.) made of ultra-low-background materials, the Compton scattering effect from gammas originating from external sources (the ground, the walls, and the atmosphere) can be minimized. As a general rule, if the detector is completely

surrounded by 4″ of lead, external gammas from the ^{238}U, ^{235}U, and ^{232}Th decay series and ^{40}K are effectively attenuated. To minimize the Compton scattering effect from cosmic rays, detectors should be housed in basements of buildings or below ground. A thin copper liner is often used to separate the detector (and sample) from X-rays generated by the lead shielding itself.

In general, the larger the scintillation or Ge Detector (in thickness and surface area), the higher the efficiency for the ^{7}Be detection process, but larger detectors require the thickest shielding. The efficiency of the detector type for absorbing the full energy of the 478 keV ^{7}Be gamma is a function of the detector and the counting geometry. The relationship between efficiency and energy for each detector and counting geometry must be defined to calculate accurate ^{7}Be concentrations. This is commonly done by counting a synthesized mixture of radionuclides that decay over a wide range of energies (40–1,400 keV) in the exact geometry that the unknown samples will be analyzed in, which allows the analyst to construct a relationship between energy (keV) and detection efficiency. Alternately, if certified ^{7}Be Standard Reference Material can be obtained, then, the detector can be calibrated for well-defined geometries and dpm/cpm ratios can be obtained for different geometries and these ratios can be directly used to obtain the activities of samples. Detectors can be planar in form for petri-dish style counting geometries, but large well detectors have the highest efficiencies for small geometry samples (a Ge well detector has an absolute detection efficiency at 478 keV of 21.9 $\pm$ 0.3% for 1-mL geometry; Jweda et al. 2008). There have been successful measurements of ^{7}Be in environmental samples by accelerator mass spectrometry, which has a detection limit of ~10^{4} atoms (corresponding to 0.09 dpm or 1.5 mBq) which is at least an order of magnitude more sensitive than the counting methods (Nagai et al. 2004). Details on calculation of activities and calibration methods are given in Baskaran et al. (2009b).

A number of accelerators (e.g., Tandem Van De Graaff and other high-voltage Tandem accelerators, cyclotron, etc.) have been utilized to measure ^{10}Be (Raisbeck et al. 1978b; Turekian et al. 1979; Galindo-Uribarri et al. 2007). Details on the differences between these accelerated mass spectrometers are beyond the scope of this article. A detailed methodology on how the Tandem Van De Graaff accelerator is set-up and used for the ^{10}Be measurements is given in Turekian et al. (1979).

5.3 Applications

The near-steady input of ^{7}Be and ^{10}Be and the particle-reactive nature of the Be atom makes meteoric Be nuclides a very useful tracer for quantifying a range of environmental processes operating on timescales from weeks to millennia. Both nuclides can be used to study atmospheric transport and depositional processes (see Lal and Baskaran 2011, Chap. 28). ^{7}Be can be used to quantify a number of short-timescale processes, including the infiltration of particle-reactive elements in soils, overland flow processes, and topsoil erosion (see Matisoff and Whiting 2011, Chap. 25). In lakes, streams, and marine environments, ^{7}Be is a valuable tracer of colloid and particulate dynamics, recent sediment deposition, mixing and focusing, and particle resuspension and transport. Meteoric ^{10}Be has been used to quantify landform age, creep rates, erosion rates, loess accumulation, and it has potential for dating authigenic mineral formation.

5.3.1 Using ^{7}Be and ^{10}Be to Trace Hillslope and Soil Processes

The short half-life of ^{7}Be makes it a valuable tracer of event-scale transport in soil profiles and on hillslopes. Given that ^{7}Be is usually deposited during rainfall events, especially intense rains and thunderstorms, the vertical distribution of this nuclide in soils can be used to infer the initial depth-penetration of other particle-reactive radionuclides and contaminants from a single deposition event. The initial conditions for an advection-diffusion transport model of other fallout isotopes (e.g., ^{210}Pb) can be constrained using the vertical distribution of ^{7}Be (Kaste et al. 2007). Measurements of ^{7}Be in stormwater, for example, can be used to study the fate of atmospherically-deposited particle reactive contaminants (Hg, Pb, etc.) released from a melting snowpack (Cooper et al. 1991). The spatial distribution of ^{7}Be on hillslopes measured after a significant storm can also be used to trace

event-scale soil sediment redistribution. If the ^{7}Be distribution is compared with the distribution of other sediment tracers that track longer timescales (e.g., ^{137}Cs), the contribution of single, intense storms to soil movement can be put into perspective with processes operating over the course of years to decades (Walling et al. 1999).

Because of its longer half-life, meteoric ^{10}Be has great potential for quantifying soil and sediment transport processes and authigenic mineral formation rates on soil-mantled hillslopes (Willenbring and von Blanckenburg 2010a). The inventory of meteoric ^{10}Be (I, in units of atoms area^{-1}) at a point on Earth can be expressed as:

$$I = \int_{-z}^{0} C\rho \, dz \tag{5.2}$$

where $-z$ is the depth in the soil to which meteoric ^{10}Be has penetrated, 0 is the soil surface, C is the concentration of meteoric ^{10}Be (in atoms mass^{-1}), and ρ is the soil density (mass volume^{-1}). In practice, this is measured by collecting samples with sampling depth resolution (dz) on the order of 20 cm to up to a meter (Pavich et al. 1985; McKean et al. 1993; Jungers et al. 2009). The inventory I at a location is governed by ^{10}Be deposition, which is a function of production in the atmosphere and wet + dry depositional processes, age, radioactive decay, particulate losses, and solute losses. Inventories are used to find the age of stable, non-eroding surfaces if the nuclear production rates in the atmosphere and deposition varies around some mean value that can be constrained for time period of interest (Tsai et al. 2008; Willenbring and von Blanckenburg 2010a). However, at many sites, solution and/or erosional losses limit the ^{10}Be inventories (Monaghan et al. 1983). Given an eroding surface where weathering, soil formation, and soil loss are in equilibrium, inventories can be used to calculate steady-state erosion rates (Pavich et al. 1986; Brown et al. 1988). This technique can be extended to study the fate of other particle-reactive elements on landscapes. For example, the loss and accumulation of ^{10}Be over different points of a landform can be used to study how sediment transport processes control the fate and storage of carbon on a hillslope (Harden et al. 2002).

Inventories of meteoric ^{10}Be along points on soil-mantled hillslope profiles often increase with distance from the divide (McKean et al. 1993). This gradient results because points farthest from the divide have traveled the longest distance and resided on the hillslope for a longer duration and thus received more of a ^{10}Be dose. By constructing a linear regression between I values measured for points on a hillslope profile and projected soil particle paths, Jungers et al. (2009) used the rate of inventory change (dI/dx) and an average ^{10}Be input assumption to calculate virtual soil velocities for a hillslope in the Great Smoky Mountains, NC. Downslope soil transport velocities calculated using ^{10}Be inventories can be used to test assumptions about landscape equilibrium. McKean et al. (1993) used this technique to show that the soil creep flux was related to slope, which supported G.K. Gilbert's hypothesis (1877) that hillslopes exist in a dynamic equilibrium with a uniform soil production rate.

Meteoric ^{10}Be may be useful for dating authigenic minerals in soils, which was first suggested by Lal et al. (1991). Dating of secondary minerals in soil profiles could be extremely valuable for quantifying the rate of soil formation, and, using additional information, can be used for putting formation rates into context with erosion rates. Secondary minerals have, for the most part, defied traditional isotopic dating methods, such as U-Th series chronology, because of large uncertainties in defining the initially inherited isotopic composition (Cornu et al. 2009).

Barg et al. (1997) developed a "closed system" model which relied on the ^{10}Be/^{9}Be ratio as a chronometer for modeling the age of clays and iron and aluminum hydroxide minerals. In this model, cosmogenic ^{10}Be and bedrock-derived ^{9}Be equilibrate in the upper soil horizons, and slowly move down the profile by adsorption-desorption reactions. It is assumed that secondary minerals form primarily in the C-horizon, and, at the time of formation ^{10}Be/^{9}Be is locked in, and will change as a function of time. Indeed, the ^{10}Be/^{9}Be values were found to be in a narrower range than the ^{10}Be concentration, and, by using selective chemical extractions that targeted secondary minerals, they found that the highest ^{10}Be/^{9}Be values were found at the soil-bedrock interface, where authigenic mineral formation is projected to take place. This technique needs considerably more development, to account for secondary mineral dissolution and illuviation processes.

5.3.2 Using ^{7}Be as a Tracer in Lake and River Systems

5.3.2.1 ^{7}Be as a Tracer of Metal Scavenging, Colloidal, and Particulate Dynamics in Lakes

When dissolved metals are introduced into lake waters via atmospheric deposition, they can be scavenged by colloids, a process that greatly reduces their potential toxicity to the lake's ecosystem. Honeyman and Santschi (1989) describe a "colloidal pumping" process by which metals are removed from waters in three stages: (1) in the first stage, dissolved trace metals and radionuclides are released into the water column, either from atmospheric deposition or through production from the parents and these species are removed quickly onto colloidal particles through sorption reactions; (2) colloidal-bound trace metals and radionuclides undergo coagulation relatively slowly with the small particle pool and (3) the particles move in the particle size spectrum and are then eventually removed from the water column. In this, the coagulation of colloids is the rate controlling step in trace metals and radionuclide scavenging. Steinmann et al. (1999) modified a steady-state particle scavenging model (Honeyman and Santschi 1989) so that (λ = 0.013 d^{-1}, the decay constant of ^{7}Be) ^{7}Be could be applied to study mechanisms and rates of metal scavenging from the waters of Lake Lugano (Switzerland, Italy):

$$\begin{aligned} Be_d\lambda_{ads} &= Be_c\lambda + Be_c\lambda_{coag} \\ Be_c\lambda_{coag} &= Be_p\lambda + Be_p\lambda_{sed} \\ F_{sed}^{Be} &= Be_p\lambda_{sed} \end{aligned} \qquad (5.3\text{-}5.5)$$

By directly measuring the concentrations (in Bq m^{-3}) of dissolved ^{7}Be (Be_d; <10 kD), colloidal ^{7}Be (Be_c; 10 kD–1 μm), particulate ^{7}Be (Be_p; >1 μm), and the sedimentary flux of ^{7}Be ($F_{sed;}^{Be}$ in Bq m^{-3} day^{-1}), the adsorption rate (λ_{ads}) of ^{7}Be onto colloids was calculated to be approximately 0.02–0.005 day^{-1}, corresponding to a dissolved ^{7}Be residence time of 50–200 days. The residence time of colloids ($1/\lambda_{coag}$) ranged from a few days to a few weeks, while the residence time of particulates ($1/\lambda_{sed}$) was typically less than a week. The authors suggested that colloids <10 kD containing ^{7}Be could be affecting the calculated residence times, and thus adsorption rates of ^{7}Be, and that perhaps the rate limiting step for the removal of Be from the water column was in fact the coagulation of small colloids <10 kD. This application of ^{7}Be was also useful for quantifying the effect of biological processes on trace metal scavenging, as the highest coagulation rates (λ_{coag}) followed algal blooms. While true steady-steady conditions may not be possible on timescales of weeks because of the episodic nature of ^{7}Be deposition, the quantitative modeling approach described above is still useful for constraining the rates of metal adsorption, colloidal coagulation, and particle sedimentation in natural systems (Dominik et al. 1989).

^{7}Be can also be used to identify sources of particulates to the water column in lakes and to examine mixing processes. In Lake Michigan, under isothermal conditions that persist from December to May, the concentration of ^{7}Be on suspended matter is nearly constant with depth (Robbins and Eadie 1991), indicating that the waters are mixed vertically on short timescales.

However, in early summer, the ^{7}Be content of suspended sediments reaches a maxima near the surface of the lake (<20 m) as lake stratification limits the settling of sediment (Robbins and Eadie 1991). A similar stratification effect on the vertical distribution of ^{7}Be has been observed in waters of Lake Zurich (Schuler et al. 1991). In the summer, calcite formation and/or algal blooms can effectively scavenge ^{7}Be from the upper fraction of the water column, reducing ^{7}Be in the epilimnion (Robbins and Eadie 1991; Vogler et al. 1996). In the late fall, lake turnover recharges the suspended sediment pool to lake water again, as ^{7}Be increases again in the epilimnion (Robbins and Eadie 1991; Vogler et al. 1996). These tracer studies have demonstrated how the dissolved to particulate ^{7}Be varies seasonally, and that the scavenging of metals from surface waters can be controlled by biological productivity and/or authigenic mineral formation.

5.3.2.2 ^{7}Be as a Tracer of Sediment Source, Focusing, Resuspension, and Transport in Rivers

Sediment can directly and indirectly degrade river ecosystems, and humans have altered landscapes and sediment fluxes and dynamics in nearly every river system on Earth. The focusing of fine sediment deposition from land use change, in particular, can degrade

spawning gravels, and, in some cases, sediments contain particle-reactive contaminants such as Pb, Hg, and PCBs that directly impact organisms. Cosmogenic ^{7}Be can be a useful tracer in fluvial systems, and has been successfully used to trace sediment sources in rivers, residence times, resuspension rates, transit times, and the fate of recently contaminated sediments. In many cases the use of ^{7}Be in fluvial systems relies on the fact that sediments that are buried for a period of more than 6 months will have undetectable ^{7}Be. This "old" sediment can be separated from recently exposed sediment by doing end-member mixing analysis (Bonniwell et al. 1999; Matisoff et al. 2005). In rivers, sediment deposition and resuspension rates can be calculated by projecting the inventories present in bed sediments present from atmospheric deposition, and quantifying depletion from resuspension, or excess, from deposition (Jweda et al. 2008). This technique was used in the Fox River, in Wisconsin, to determine the fate and dynamics of a PCB-contaminated sediment layer (Fitzgerald et al. 2001), much of which was resuspended during high flow despite the impounded nature of the river.

Humans have profoundly altered the flow regimes and sediment supplies of rivers through urbanization, logging, the construction of dams, and the engineering of stream banks (Croke et al. 1999; Magilligan et al. 2003). In recent years, the use of ^{7}Be as a tracer of fine sediment deposition, resuspension, and transport has been expanded to study processes in a wide range of fluvial environments, and to quantify how sediment dynamics might respond to different forcings. The enrichment of the upper few cm of topsoil with ^{7}Be makes it a valuable tracer of sediments derived from surface erosion (Blake et al. 1999, 2002; Wallbrink et al. 1999) and enables a quantitative partitioning of runoff processes between sheetwash and rilling (Whiting et al. 2001). Sediment transport rates within a fluvial system can also be calculated using ^{7}Be. Salant et al. (2007) repeatedly measured point bar and streambed sands in a regulated river immediately downstream of a dam in Vermont, U.S.A. During the winter months, sediment stored behind the dam became depleted in ^{7}Be, and when the gates were opened in the early spring the pulse of depleted "new" sediment was discernable from the surrounding sediments that were supplied by tributaries and previously exposed bars. Sediment transport rates of 30–80 m day^{-1} were calculated using the known starting point of the sands and monthly sampling at fixed points to monitor the pulse of sediment as it moved down river. The ^{7}Be content of bedload sediment in a single river varies by more than a factor of two over the course of a single year, as seasonal changes in ^{7}Be delivery (Olsen et al. 1985) and flow regimes regulate sediment source, grain size, and transport processes. Cosmogenic ^{7}Be may trace sediment substrates and nutrients that are favorable for certain aquatic insects. Svendsen et al. (2009) reported a significant correlation between ^{7}Be concentrations in transitional bed load sediment and benthic community structure at tributary junctions along a mainstem river in Vermont.

There is a strong dependence of grain size on the adsorption of ^{7}Be, and, in rivers, grain size will vary with flow regime which can make the relationship between ^{7}Be and age difficult to reconstruct. To normalize for grain-size effects on ^{7}Be values, models have been developed that utilize the ^{7}Be/^{210}Pb$_{ex}$ ratio for calculating sediment age or fraction of new sediment in suspension. This relies on the fact that ^{210}Pb$_{ex}$, which is the atmospherically-delivered portion of ^{210}Pb in sediments (^{210}Pb in "excess" of that projected to be supported by in situ ^{222}Rn decay) also adsorbs strongly to sediment and organic matter surfaces, and is reported to have partitioning coefficients (K_d) at least as high as Be (Sauve et al. 2000a, b). The change in the ^{7}Be/^{210}Pb$_{ex}$ can thus be a more sensitive indicator of age, since ^{7}Be decays much faster than ^{210}Pb. Others have found a very strong correlation with ^{7}Be/^{210}Pb values and ^{7}Be divided by grain surface area (Fisher et al. 2010). In a study of a coastal plain river in Maine, U.S.A., Fisher et al. (2010) used a constant initial ^{7}Be/^{210}Pb model to measure the timescale of sediment storage behind large woody debris and boulders. They found that in independently-assessed "transport-limited" reaches of the Ducktrap River, sediment sequestration behind in-stream obstructions was >100 days, but in supply limited reaches sediment was replenished more quickly.

5.3.3 Applications of Meteoric ^{7}Be and ^{10}Be as Process Tracers in the Marine Environment

From the time the ^{7}Be and ^{10}Be are produced in the atmosphere until its ultimate disposal, either through radioactive decay or their permanent incorporation into

the bottom sediments in oceans, these nuclides often pass through a number of transient reservoirs, such as various layers of atmosphere, precipitation and surface waters. The half-life of ^{7}Be is suitable for studying the vertical eddy diffusion coefficients and associated vertical transport rates in the upper layers of the thermocline (Silker 1972; Kadko and Olson 1996). Silker (1972) utilized the vertical concentration gradients of ^{7}Be in the Atlantic water column to determine the vertical eddy diffusion coefficients within the thermocline, assuming that atmospheric input of ^{7}Be is constant and the horizontal advective transport is negligible. Due to its short mean-life (76.9 days) and the lack of biological removal of Be, the effects of long-range advective transport on the vertical distribution is likely negligible and hence it is reasonable to assume that ^{7}Be will be effective in tracing diffusion at the top of the thermocline. Since^{7}Be is delivered at the air-water interface, that layer is "tagged" with ^{7}Be constantly and when this layer undergoes sinking, the vertical profiles of ^{7}Be can be utilized to retrieve the record of the seasonal changes in the mixed layer depth (Kadko 2000).

5.3.3.1 Measuring Sediment Accumulation, Mixing Rates, and Sediment Focusing with ^{7}Be

A large number of studies have been conducted utilizing ^{7}Be to identify and quantify flood deposits (Corbett et al. 2007; more discussion are given in Du et al. 2011, Chap. 16). ^{7}Be is also utilized to quantify recent sediment accumulation and mixing rates (Krishnaswami et al. 1980; Clifton et al. 1995; Corbett et al. 2007). The sediment mixing involves both advective (physical particle transport) and diffusive mixing components. A combined effect of advective and diffusive mixing is analogous to eddy diffusion and has been modeled to determine eddy mixing coefficients. In coastal areas, the ^{7}Be profiles in sediments are not often in steady-state due to seasonal variations in the riverine discharge which delivers relatively large amount of ^{7}Be. In marine and lacustrine environments, the sediment inventories at selected sites are often far excessive compared to what is expected and this elevated levels is often caused by physical transport processes of sediments (such as sediment focusing by bottom currents and gravity flows, e.g., slumps and gravity flows). A comparison of the measured sediment inventories (I_{sed}, Bq m^{-2}) to the measured depositional fluxes (or expected) of ^{7}Be (I_{dep}) will yield information on sediment focusing ($I_{sed}/I_{dep} > 1$) or erosion ($I_{sed}/I_{dep} < 1$).

5.3.3.2 Boundary Scavenging and Long-Range Transport of ^{10}Be in Marine Systems

Advective transport of dissolved nuclides to regions of high productivity waters in the margins results in higher suspended particle concentrations and fluxes which result in enhanced scavenging of ^{10}Be and other particle-reactive nuclides (e.g., ^{230}Th, ^{231}Pa, ^{210}Pb, etc.). In ocean margin sediments, the ^{10}Be concentrations were found to be much higher than that expected from the direct atmospheric deposition and this was attributed to boundary scavenging. The deposition rates of ^{10}Be in pelagic red clays were reported to be much less than its global average production rate, whereas in ocean-margin sediments, the ^{10}Be deposition rate exceeds its global average production rate (Brown et al. 1985; Anderson et al. 1990; Lao et al. 1992b). Particle composition (such as opal Si, Fe-Mn oxides, carbonate, terrigenous material such as clays; Luo and Ku 2004a, b; Chase et al. 2003) also plays a significant role on the scavenging of dissolved ^{10}Be. Sharma et al. (1987) reported strong correlation between ^{10}Be and Al in the sediment trap and attributed the aluminosilicate to be the major carrier phase for the scavenging of dissolved ^{10}Be.

Deposition rates of ^{10}Be at margin sites calculated from sedimentary records (= sediment accumulation rates (g cm^{-2} year^{-1}) × concentration of ^{10}Be in surficial sediments (atoms g^{-1})) have been found to be significantly higher than the rate of ^{10}Be supply at the Earth's surface at sites far away from the margins (such as off Northwest Africa and off California, equatorial Pacific off Ecuador, margins in North Atlantic, Brown et al. 1985; Anderson et al. 1990) and is attributed to boundary scavenging. Boundary scavenging exerts influence when the dissolved residence time of Be is greater than the time required for the advective transport to move the water from the center of the basin to the margins. Physical transport processes such as bottom currents and gravity flows (turbidities and slumps) also could lead to increased rates of ^{10}Be accumulation rates, resulting in higher ocean-wide average ^{10}Be deposition rates.

There are limited data on the temporal and spatial variations of ^{10}Be and ^{7}Be isotopes in oceanic particulate matter. Depositional fluxes measured in sediment traps deployed at two sites in the eastern equatorial North Pacific Ocean show that the ^{10}Be flux at traps deployed 50 m above the bottom of the sediment-water interface were up to an order of magnitude higher than that at mid-depth in the water depth column (at 1,565 and 1,465 m with total water of 3,100 and 3,600 m). The flux in the bottom trap (4.6×10^{6} and 2.4×10^{6} atoms cm^{-2} year^{-1}) was significantly higher than the average global depositional flux of 1.2×10^{6} atoms cm^{-2} year^{-1} while at intermediate depth the ^{10}Be flux was lower (0.9×10^{6} and 0.4×10^{6} atoms cm^{-2} year^{-1}) than the global depositional flux (Sharma et al. 1987). This difference was attributed to contribution from lateral input as well as from the resuspended material in the bottom nepheloid layers. A strong correlation between ^{10}Be concentration and Al suggest that aluminosilicate is the major carrier phase of ^{10}Be. Variations in atmospheric dust input may result in variations in the scavenging of ^{10}Be from the water column and thus, the variations in particle fluxes can be linked to the depositional fluxes in the traps.

5.3.3.3 ^{7}Be as a Tracer of Ice Rafted Sediments (IRS) in the Oceans

Concentrations of ^{7}Be in ice-rafted sediments (IRS) in the seasonal ice-cover of the Arctic Ocean have been reported to be relatively high (Masque et al. 2007). When sea ice is formed mostly in shallow waters in the marginal seas of the Arctic Ocean (such as Siberian margins of the Laptev, Kara and Barents Seas), large amounts of fine-grained sediments get incorporated into the sea ice during formation of new ice mainly through suspension freezing of bottom sediments and river-borne sediments (Barnes et al. 1982; Reimnitz et al. 1992; Nurnberg et al. 1994) and are subsequently transported to different parts of the Arctic. During its transit, atmospherically-delivered ^{7}Be is intercepted by the ice cover and the ^{7}Be is added to the IRS during freezing-thawing cycles (Baskaran 2005). The activities of ^{7}Be in IRS have been reported to be highly variable, with values ranging between $10^{4.9}$ and $10^{6.2}$ atoms g^{-1} (13 and 212 Bq kg^{-1}), which is 1–2 orders of magnitude higher than those reported in the coastal sediments. The dissolved ^{7}Be activities in melt ponds were also reported to be much higher (30–60 mBq L^{-1}) than the surface waters in the Arctic (0.6–2.3 mBq L^{-1}) as well as surface water samples collected between 1.0 and 2.0 m from the air-sea interface (2.6 mBq L^{-1}) (Eicken et al. 2002; Kadko and Swart 2004). The concentrations of ^{7}Be in sea ice also were reported to be ~2 orders of magnitude higher than that in the ocean mixed layer below the sea ice and this was attributed to dilution of ^{7}Be with longer depths of the mixed layer compared with the <1 m thick seasonal ice (Cooper et al. 1991). During summer, the snow and upper 0.3–0.7 m of the ice melt off the ice surface. Tracer studies indicate that meltwaters disperse over distances of tens of meters on time scales of days, with much of the meltwater pooling in depressions at the surface (Eicken et al. 2002). IRS accumulates at the surface and in melt pools and are subjected to meltwater flushing (Nurnberg et al. 1994). During this process, the IRS released from melting comes in contact with seawater in meltponds and additional scavenging may take place. It has been estimated that ~60% of the ^{7}Be inventory is found in the water column from the sea ice melt and the remaining ~40% in found in sea ice (Eicken et al. 2002). Based on controlled experiments, it has been estimated that ~15% of the total sediment load is released to the water column during melt (Eicken et al. 2002). During multiple freezing-thawing cycles, the IRS is often pelletized and thus, can undergo sinking very quickly. Cooper et al. (2005) reported ^{7}Be in benthic surface sediments collected as deep as 945 m in Barrow Canyon in the Arctic, but it has not been reported from any other ocean basins. The activities of ^{7}Be in benthic sediments at different water column depths will be useful to quantify the amount of sediments released from melting of sea ice.

5.3.3.4 Using Meteoric ^{10}Be as a Chronological Tool in Marine Sediments

^{10}Be has been extensively utilized to date marine sediments, Mn-nodules, and other authigenic minerals. Prior to the development of AMS techniques, dating of Mn-nodules and deep-sea sediment cores were dated by conventional beta counting technique (Somayajulu 1967; Sharma and Somayajulu 1982). The concentration of ^{10}Be in Mn-nodules is very high (~10^{10} atoms g^{-1}) and hence a very small amount of sample is required (<10 mg). The first measurement of

^{10}Be by AMS basically confirmed the slow growth rates of Mn-nodules observed by conventional counting method (Somayajulu 1967; Turekian et al. 1979). Based on the exponential decay of ^{10}Be with depth on manganese crusts over a period of past 7 Ma, Ku et al. (1982) suggested that the ^{10}Be/^{9}Be ratio has remained constant over this time period. The ^{10}Be concentrations in Mn-nodules extrapolated to zero depth indicate that there is wide range of ^{10}Be values in nodules collected at different basins and varied between 1.5×10^{10} and 6.5×10^{10} atoms g^{-1} (Kusakabe and Ku 1984; Segl et al. 1984a, b; Mangini et al. 1986). The ^{10}Be/^{9}Be ratios in nodules from Atlantic and Pacific only ranged between 1.1×10^{-7} and 1.6×10^{-7}. A comparison of the extrapolated to the surface value (corresponding to present time) of ^{10}Be/^{9}Be ratio to that in the deep waters suggesting that the dissolved Be are well mixed in the bottom waters and that the ratio is well-preserved in authigenic minerals formed out of seawater (Kusakabe et al. 1987). Sediment cores have been dated using certain assumptions that include constant supply of ^{10}Be to the seafloor over the time interval of interest. It has been shown that the flux of ^{10}Be is largely dependent on the sedimentation rate (Tanaka et al. 1982; Mangini et al. 1984). Sediment focusing and boundary scavenging, however, make the assumption of constant supply of ^{10}Be questionable. In the Arctic, the variations in the particle flux (due to variations in the release of ice-rafted sediments) have resulted in highly varying concentrations of ^{10}Be in a vertical profile (Eisenhauer et al. 1994; Aldahan et al. 1997). The authigenic minerals seems to be better candidates for ^{10}Be dating compared to deep sea sediments, as the chemical link between deep seawater and authigenic minerals make this method work well for authigenic minerals. By measuring the ^{10}Be in deep-ocean Fe-Mn crusts, the decay corrected ^{10}Be/^{9}Be ratio was found to be constant over the past 12 Myr and this was attributed to constant global chemical weathering flux over this time period (Willenbring and von Blanckenburg 2010b).

5.3.3.5 Case Study: Dating of Marine Particulate Matter Using ^{7}Be/^{10}Be Ratios as Tracer

As was discussed earlier, once ^{7}Be and ^{10}Be are delivered at the air-sea interface primarily through wet precipitation, during their life-span in the water column, they are scavenged by suspended particulate matter and eventually reach the ocean floor. Due to the short mean-life of ^{7}Be, most of the ^{7}Be undergoes radioactive decay while virtually no ^{10}Be undergoes radioactive decay. Although there are more than an order of magnitude variations on the monthly depositional fluxes of these nuclides, the variations on the ^{7}Be/^{10}Be ratios is very narrow, within a factor of ~2 (Brown et al. 1989; Graham et al. 2003; Heikkila et al. 2008; Lal and Baskaran 2011). When marine particulate matter leaves the surface layer with a finite ^{7}Be/^{10}Be ratio, as it sinks the ratio values will decrease and the rate of decrease can, in principle, be used to date the marine particulate matter, provided additional scavenging of ^{7}Be and ^{10}Be in subsurface layers does not alter the ^{7}Be/^{10}Be ratio. With the detection limit of ^{7}Be of 10^{4} atoms using AMS (Raisbeck and Yiou 1988), one can measure ^{7}Be/^{10}Be ratios in particulate matter collected from ~20 L water sample assuming that 0.2 Bq/100 L of ^{7}Be (2.65×10^{5} atoms), the average value for a six coastal water systems along the Gulf coast (Baskaran and Santschi 1993; Baskaran et al. 1997; Baskaran and Swarzenski 2007) and ^{10}Be abundance of ~500 atoms g^{-1} (corresponding to ~10^{7} atoms of in 20-L sample), particulate matter can be reliably dated.

When particles leave the mixed layer with ^{7}Be/^{10}Be ratio (R_0), at any depth below mixed-layer, the measured ratio is R_d, then the time of transit (or residence time) of particulate matter is given by:

$$t = \tau \ln(R_0/R_d) \tag{5.6}$$

where τ is the mean-life of ^{7}Be. If we assume that the particles are fresh in the mixed-layer, then, t can be considered as the age of the particulate matter. At depth "d," if there is equilibrium between the particulate matter and dissolved phase, then, the dissolved phase will likely have the same ^{7}Be/^{10}Be ratio as the particulate matter and hence by measuring ^{7}Be/^{10}Be ratio in the dissolved phase, we will be able to determine the "age" of the particulate matter.

5.3.4 Other Applications of Meteoric ^{7}Be and ^{10}Be at the Earth's Surface

The unique source term of the ^{7}Be and ^{10}Be nuclides make them particularly useful for tracing deposition and examining whether minerals are formed from elements derived from the atmosphere or the lithosphere.

Recently, these nuclides were used to study how rock varnish accumulates elements (Moore et al. 2001). Rock varnish specimens shielded from rainfall accumulate detectable ^{7}Be, presumably from dew or dry deposition, but specimens exposed to precipitation accumulate considerably higher doses of ^{7}Be. It was calculated that rock varnish accumulates a few percent of the total deposition of cosmogenic Be nuclides; ultraviolet radiation did not inhibit ^{7}Be accumulation in rock varnish, which suggests that varnish may be formed abiotically (Moore et al. 2001). The use of cosmogenic Be isotopes in conjunction with other fallout radionuclides (^{137}Cs, ^{210}Pb) may be useful for understanding the rates and mechanisms by which atmospheric elements are incorporated into mineral structures (Fleisher et al. 1999; Moore et al. 2001).

5.4 Other Future Directions

5.4.1 Deposition

There is considerable uncertainty on how cosmogenic Be deposition varies spatially over the Earth's surface and how climate might control fluxes to points on land and sea. The meteoric input uncertainty appears to be limiting our ability to quantify and compare the residence time of dissolved Be radionuclides in the oceans (Table 5.3). Climate change will likely result in the global redistribution of rainfall, and changes in the frequency and intensity of rainfall may affect the seasonal depositional fluxes of meteoric Be. However, input functions need to be well constrained in order to effectively use ^{7}Be and ^{10}Be as tracers in the environment, and, in particular, to apply ^{10}Be to quantify ages or steady-state erosion rates on timescales of thousands to millions of years. While there is often an inverse relationship between ^{7}Be and ^{10}Be concentrations in rainfall and storm duration at many sites (Baskaran et al. 1993; Baskaran 1995; Ishikawa et al. 1995), the dependence of annual cosmogenic Be fluxes on precipitation rates has not been well described. If cosmogenic Be is removed from an air mass during the initial parts of a storm, as most datasets indicate, a question remains as to whether or not additional rainfall over some threshold has an additive effect on fluxes. A number of studies have demonstrated that rainfall rates ultimately control the total amounts of tropospheric contaminants and weapons-derived atmospheric ^{137}Cs delivered to the surface (Kiss et al. 1988; Simon et al. 2004). However, Willenbring and Von Blanckenburg (2010a) suggested that at coastal and island settings where the atmospheric transport time is fast and ^{10}Be and ^{7}Be concentrations in rain have a strongly inverse relationship with precipitation rate, annual fluxes should remain constant even if climate were to vary. The controls that climate and annual precipitation have on cosmogenic Be nuclide deposition should be studied further.

There are essentially two methods by which annual atmospheric fluxes can be determined for a region: direct monitoring of wet + dry atmospheric deposition on a weekly to monthly basis, or indirect determination using soil, sediment, and/or ice inventories. Long-term monitoring of cosmogenic Be wet depositional fluxes on landscapes can be costly, and it can be difficult assessing dry fluxes. The use of stable surfaces that record cosmogenic Be inventories has some advantages for calculating fluxes if surface age is known or if steady-state can be assumed. Relating ^{10}Be inventories to atmospheric fluxes would be complex given that surface age, and solute and particulate losses would be difficult to constrain in everything but perhaps ice records, but the use of ^{7}Be for this purpose does not suffer from these complications. The advantage of using surface inventory measurements of ^{7}Be for calculating fluxes is that a single measurement can integrate months of deposition, which works particularly well in temperate climates where rainfall is generally evenly distributed throughout the year. At sites where there is a distinct wet and dry season, multiple samples may be necessary to calculate annual atmospheric fluxes. There is an order of magnitude range of ^{7}Be soil inventories reported for stable soils around the world (Table 5.1). While many of the sites measured for ^{7}Be inventories are of temperate climate, the one arid region dataset falls in the low end of the range, reporting approximately 85 Bq m^{-2} for Owens Valley, CA (Elmore et al. 2008). Salisbury and Cartwright (2005) used ^{7}Be measurements of sheep feces to infer that vegetation along an elevation gradient in North Wales had higher concentrations of ^{7}Be. While they could not calculate atmospheric fluxes from their measurements, their data indicate some relationship between wet precipitation amounts and cosmogenic Be deposition. It would be valuable to have surface ^{7}Be inventory data available

for a range of climates so that that processes controlling atmospheric fluxes could be better understood.

5.4.2 Species and Geochemical Behavior

The geochemical behavior of Be is complex, yet simplifications are often made in order to extend the use of ^{7}Be and ^{10}Be as process tracers. It is evident from experimental work that partitioning strength is generally high ($K_d > 5{,}000$), but dissolved meteoric Be is commonly measurable or even dominates over particle-bound Be in the water columns of lakes and oceans (Silker et al. 1968; Kusakabe et al. 1982, 1987, 1990; Bloom and Crecelius 1983; Sharma et al. 1987; Dibb and Rice 1989a; Dominik et al. 1989; Steinmann et al. 1999). It appears that the availability of particles in a water column may limit the scavenging of meteoric Be radionuclides, but the effects of salinity, time, and particle composition (e.g., algae, organic detritus, Al/Fe/Mn phases) on partitioning strength and kinetics need to be better quantified.

In neutral to alkaline soil environments, Be is expected to form complexes with oxygen on surfaces of secondary clays and oxides and organic matter (Nyffeler et al. 1984; You et al. 1989). However, it is possible that soluble Be complexes could form, inhibiting adsorption and increasing the geochemical mobility of ^{7}Be and ^{10}Be in the environment. Equilibrium thermodynamic approach has been used to predict that Be forms soluble complexes with humic and fulvic acids and fluoride (Vesely et al. 1989; Takahashi et al. 1999) but there are no field-based studies documenting enhanced mobility in the environment from these species. It is also possible that cosmogenic Be could adsorb to very small colloids formed at soils through the breakdown of organic matter and Be could migrate vertically downward. Steinmann et al. (1999) used continuous flow centrifugation and tangential flow ultrafiltration to separate dissolved, colloidal, and particulate ^{7}Be phases in lake water. Despite their substantial efforts to separate truly dissolved ^{7}Be from other phases, they concluded that ^{7}Be might be adsorbed to very fine colloids ($<$10 kD) that are not easily separated from other phases or size fractions. More theoretical, experimental, and field-based data need to be collected on the distribution of Be species in the environment, and to identify the various mechanisms by which cosmogenic Be can be transported in different systems.

5.4.3 "Dating" of Suspended Particulate Matter with ^{7}Be/^{10}Be

Particulate matter at the air-sea interface is tagged with a finite ^{7}Be/^{10}Be ratio which is likely to remain constant at any season and as the particles undergo sinking, ^{7}Be undergoes radioactive decay. Typical settling rates of a terrigenous particle (density = 2.6 g cm^{-3}) of 4 mm diameter is ~1 m day^{-1} (for 16 mm diameter ~19 m day^{-1}, corresponding to reaching a depth of ~1,460 m over the mean-life of ^{7}Be). Particulate matter from a sediment trap deployed at ~1,500 m can be utilized to determine the settling velocity of particulate matter. ^{7}Be/^{10}Be measurements on size-fractionated particulate matter could provide differences in the settling velocity of particulate matter. The deposition velocities could provide insight on the particle aggregation-disaggregation processes that are taking place in marine environment. It is known that beryllium is biologically inactive and hence could serve as an ideal tracer for the settling of terrigenous particulate matter. In the Arctic, ^{7}Be/^{10}Be ratios in sediment traps from seasonally ice-covered areas could provide insight on the amount of sediments released from sea ice during seasonal melting-freezing cycles. While ^{7}Be in sea ice sediments records the history of the material for $<$1 year, ^{10}Be data would record a much longer history, and hence the ^{7}Be/^{10}Be ratio may provide information on the time scale and extent of recycling of IRS. There are currently no ^{10}Be data available for sea ice sediments, so more work is needed to develop this potentially valuable tracing tool.

5.5 Concluding Remarks

Meteoric ^{7}Be and ^{10}Be are valuable tracers that can be used to characterize an incredibly wide range of environmental processes. While ^{7}Be can be used to quantify short-timescale processes, including the scavenging of metals and particles from waters, and the origin and fate of fine grained sediments in terrestrial and marine systems, meteoric ^{10}Be can be used to date

geomorphic surfaces and authigenic minerals, test quantitative theories about landscape evolution, and study boundary scavenging processes. However, a considerable amount of fundamental work still needs to be done to effectively use these isotopes of beryllium as tools to study Earth systems processes. The atmospheric fluxes of these nuclides and the processes that control deposition need to be characterized better, and the biogeochemical behavior of these isotopes in a wide range of environments needs to be described. We are optimistic that new studies will shed further light on the dynamics of ^{7}Be and ^{10}Be in the environment, and that these tracers will continue to help scientists solve complex environmental problems in the future.

Acknowledgements We thank Jane Willenbring for a thoughtful and thorough review of the earlier version of this manuscript.

References

Aldahan AA, Ning S, Possnert G et al (1997) Be-10 records from sediments of the Arctic Ocean covering the past 350 ka. Mar Geol 144:147–162

Anderson RF, Lao Y, Broecker WS et al (1990) Boundary scavenging in the Pacific Ocean – a comparison of Be-10 and Pa-231. Earth Planet Sci Lett 96:287–304

Arnold JR, Al-Salih H (1955) Beryllium-7 produced by cosmic rays. Science 121:451–453

Baes CF, Mesmer RE (1976) The hydrolysis of cations. Wiley, New York

Barg E, Lal D, Pavich MJ et al (1997) Beryllium geochemistry in soils: evaluation of Be-10/Be-9 ratios in authigenic minerals as a basis for age models. Chem Geol 140:237–258

Barnes PW, Reimnitz E, Fox D (1982) Ice rafting of fine-grained sediment: a sorting and transport mechanism, Beaufort Sea, Alaska. J Sediment Petrol 52:493–502

Baskaran M (1995) A search for the seasonal variability on the depositional fluxes of Be-7 and Pb-210. J Geophys Res Atmos 100:2833–2840

Baskaran M (2005) Interaction of sea ice sediments and surface sea water in the Arctic Ocean: evidence from excess Pb-210. Geophys Res Lett 32:4

Baskaran M, Santschi PH (1993) The role of particles and colloids in the transport of radionuclides in coastal environments of Texas. Mar Chem 43:95–114

Baskaran M, Shaw GE (2001) Residence time of arctic haze aerosols using the concentrations and activity ratios of Po-210, Pb-210 and Be-7. J Aerosol Sci 32:443–452

Baskaran M, Swarzenski PW (2007) Seasonal variations on the residence times and partitioning of short-lived radionuclides (Th-234, Be-7 and Pb-210) and depositional fluxes of Be-7 and Pb-210 in Tampa Bay, Florida. Mar Chem 104:27–42

Baskaran M, Coleman CH, Santschi PH (1993) Atmospheric depositional fluxes of Be-7 and Pb-210 at Galveston and College Station, Texas. J Geophys Res Atmos 98: 20555–20571

Baskaran M, Ravichandran M, Bianchi TS (1997) Cycling of Be-7 and Pb-210 in a high DOC, shallow, turbid estuary of south-east Texas. Estuar Coast Shelf Sci 45:165–176

Baskaran M, Swarzenski PW, Biddanda BA (2009a) Constraints on the utility of MnO_2 cartridge method for the extraction of radionuclides: a case study using Th-234. Geochem Geophys Geosyst 10:9

Baskaran M, Hong GH, Santschi PH (2009b) Radionuclide analysis in seawater. In: Wurl O (ed) Practical guidelines for the analysis of seawater. CRC Press, Boca Raton

Berggren AM, Beer J, Possnert G et al (2009) A 600-year annual Be-10 record from the NGRIP ice core, Greenland. Geophys Res Lett 36:5

Blake WH, Walling DE, He Q (1999) Fallout beryllium-7 as a tracer in soil erosion investigations. Appl Radiat Isot 51: 599–605

Blake WH, Walling DE, He Q (2002) Using cosmogenic beryllium-7 as a tracer in sediment budget investigations. Geogr Ann Ser A Phys Geogr 84A:89–102

Bleichrodt JF, Van Abkoude ER (1963) On the deposition of cosmic-ray-produced ^{7}Be. J Geophys Res 68:5283–5288

Bloom N, Crecelius EA (1983) Solubility behavior of atmospheric Be-7 in the marine environment. Mar Chem 12:323–331

Bonniwell EC, Matisoff G, Whiting PJ (1999) Determining the times and distances of particle transit in a mountain stream using fallout radionuclides. Geomorphology 27:75–92

Bourles D, Raisbeck GM, Yiou F (1989) Be-10 and Be-9 in marine-sediments and their potential for dating. Geochim Cosmochim Acta 53:443–452

Brown L, Klein J, Middleton R (1985) Anomalous isotopic concentrations in the sea off Southern-California. Geochim Cosmochim Acta 49:153–157

Brown L, Pavich MJ, Hickman RE et al (1988) Erosion of the Eastern United States observed with ^{10}Be. Earth Surf Process Landforms 13:441–457

Brown L, Stensland GJ, Klein J et al (1989) Atmospheric deposition of Be-7 and Be-10. Geochim Cosmochim Acta 53:135–142

Brown ET, Measures CI, Edmond JM et al (1992a) Continental inputs of beryllium to the oceans. Earth Planet Sci Lett 114: 101–111

Brown ET, Edmond JM, Raisbeck GM et al (1992b) Beryllium isotope geochemistry in tropical river basins. Geochim Cosmochim Acta 56:1607–1624

Brown ET, Stallard RF, Larsen MC et al (1995) Denundation rates determined from the accumulation of in-situ produced Be-10 in the Luquillo experimental forest, Puerto-Rico. Earth Planet Sci Lett 129:193–202

Caillet S, Arpagaus P, Monna F et al (2001) Factors controlling Be-7 and Pb-210 atmospheric deposition as revealed by sampling individual rain events in the region of Geneva, Switzerland. J Environ Radioact 53:241–256

Canuel EA, Martens CS, Benninger LK (1990) Seasonal-variations in Be-7 activity in the sediments of Cape Lookout-Bight, North Carolina. Geochim Cosmochim Acta 54:237–245

Chase Z, Anderson RF, Fleisher MQ, Kubik PW (2003) Scavenging of ^{230}Th, ^{231}Pa, and ^{10}Be in the Southern Ocean (SW Pacific sector): the importance of particle flux, particle composition, and advection. Deep Sea Res Part II 50:739–768

Clifton RJ, Watson PG, Davey JT et al (1995) A study of processes affecting the uptake of contaminants by intertidal sediments, using the radioactive tracers Be-7, Cs-137, and unsupported Pb-210. Estuar Coast Shelf Sci 41:459–474

Cooper LW, Olsen CR, Solomon DK et al (1991) Stable isotopes of oxygen and natural and fallout radionuclides used for tracing runoff during snowmelt in an arctic watershed. Water Resour Res 27:2171–2179

Cooper LW, Larsen IL, Grebmeier JM et al (2005) Detection of rapid deposition of sea ice-rafted material to the Arctic Ocean benthos using the cosmogenic tracer Be-7. Deep Sea Res 52:3452–3461

Corbett DR, Dail M, McKee B (2007) High-frequency time-series of the dynamic sedimentation processes on the western shelf of the Mississippi River Delta. Cont Shelf Res 27:1600–1615

Cornu S, Montagne D, Vasconcelos PM (2009) Dating constituent formation in soils to determine rates of soil processes: a review. Geoderma 153:293–303

Crecelius EA (1981) Prediction of marine atmospheric deposition rates using total Be-7 deposition velocities. Atmos Environ 15:579–582

Croke J, Hairsine P, Fogarty P (1999) Sediment transport, redistribution and storage on logged forest hillslopes in south-eastern Australia. Hydrol Process 13:2705–2720

Dalmasso J, Maria H, Ardisson G (1987) Th-228 nuclear-states fed in Ac-228 decay. Phys Rev C 36:2510–2527

daSilva J, Machado A, Ramos MA et al (1996) Quantitative study of Be(II) complexation by soil fulvic acids by molecular fluorescence spectroscopy. Environ Sci Technol 30:3155–3160

Dibb JE, Rice DL (1989a) The geochemistry of beryllium-7 in Chesapeake Bay. Estuar Coast Shelf Sci 28:379–394

Dibb JE, Rice DL (1989b) Temporal and spatial-distribution of beryllium-7 in the sediments of Chesapeak Bay. Estuar Coast Shelf Sci 28:395–406

Doering C, Akber R, Heijnis H (2006) Vertical distributions of ^{210}Pb excess, ^{7}Be and ^{137}Csin selected grass covered soils in Southeast Queensland, Australia. J Environ Radioact 87:135–147

Dominik J, Burrus D, Vernet J-P (1987) Transport of the environmental radionuclides in an alpine watershed. Earth Planet Sci Lett 84:165–180

Dominik J, Schuler C, Santschi PH (1989) Residence times of 234Th and ^{7}Be in Lake Geneva. Earth Planet Sci Lett 93: 345–358

Du JZ, Zhang J, Baskaran M (2011) Applications of short-lived radionuclides (^{7}Be, ^{210}Pb, ^{210}Po, ^{137}Cs and ^{234}Th) to trace the sources, transport pathways and deposition of particles/sediments in rivers estuaries and coasts. In: Baskaran M (ed) Handbook of environmental isotope geochemistry. Springer, Heidelberg

Egli M, Brandova D, Bohlert R et al (2010) Be-10 inventories in Alpine soils and their potential for dating land surfaces. Geomorphology 121:378

Eicken H, Krouse HR, Kadko D et al (2002) Tracer studies of pathways and rates of meltwater transport through Arctic summer sea ice. J Geophys Res Oceans 107:20

Eisenhauer A, Spielhagen RF, Frank M et al (1994) Be-10 records of sediment cores from high northern latitudes – implications for environmental and climatic changes. Earth Planet Sci Lett 124:171–184

Elmore AJ, Kaste JM, Okin GS et al (2008) Groundwater influences on atmospheric dust generation in deserts. J Arid Environ 72:1753–1765

Feng H, Cochran JK, Hirschberg DJ (1999) Th-234 and Be-7 as tracers for the sources of particles to the turbidity maximum of the Hudson River estuary. Estuar Coast Shelf Sci 49: 629–645

Fifield LK, Wasson RJ, Pillans B et al (2010) The longevity of hillslope soil in SE and NW Australia. Catena 81:32–42

Fisher GB, Magilligan FJ, Kaste JM et al (2010) Constraining the timescale of sediment sequestration associated with large woody debris using cosmogenic ^{7}Be. J Geophys Res Earth Surf 115:F01013

Fitzgerald SA, Klump JV, Swarzenski PW et al (2001) Beryllium-7 as a tracer of short-term sediment deposition and resuspension in the Fox River, Wisconsin. Environ Sci Technol 35:300–305

Fleisher M, Liu TZ, Broecker WS et al (1999) A clue regarding the origin of rock varnish. Geophys Res Lett 26:103–106

Frank M, van der Loeff MMR, Kubik PW et al (2002) Quasi-conservative behaviour of Be-10 in deep waters of the Weddell Sea and the Atlantic sector of the Antarctic Circumpolar Current. Earth Planet Sci Lett 201:171–186

Frank M, Porcelli D, Andersson P et al (2009) The dissolved beryllium isotope composition of the Arctic Ocean. Geochim Cosmochim Acta 73:6114–6133

Galindo-Uribarri A, Beene JR, Danchev M et al. (2007) Pushing the limits of accelerator mass spectrometry. Nucl Instrum Meth Phys Res Sect B Beam Interact Mater Atoms 259:123–130

Graham I, Ditchburn R, Barry B (2003) Atmospheric deposition of Be-7 and Be-10 in New Zealand rain (1996–98). Geochim Cosmochim Acta 67:361–373

Gu ZY, Lal D, Liu TS et al (1996) Five million year Be-10 record in Chinese loess and red-clay: climate and weathering relationships. Earth Planet Sci Lett 144:273–287

Harden JW, Fries TL, Pavich MJ (2002) Cycling of beryllium and carbon through hillslope soils in Iowa. Biogeochemistry 60:317–335

Harvey MJ, Matthews KM (1989) ^{7}Be deposition in a high-rainfall area of New Zealand. J Atmos Chem 8:299–306

Hawley N, Robbins JA, Eadie BJ (1986) The partitioning of beryllium-7 in fresh-water. Geochim Cosmochim Acta 50:1127–1131

Heikkila U, Beer J, Alfimov V (2008) Beryllium-10 and beryllium-7 in precipitation in Dubendorf (440 m) and at Jungfraujoch (3580 m), Switzerland (1998-2005). J Geophys Res Atmos 113:10

Honeyman BD, Santschi PH (1989) A brownian-pumping model for oceanic trace-metal scavenging – evidence from Th-isotopes. J Mar Res 47:951–992

Husain L, Coffey PE, Meyers RE et al (1977) Ozone transport from stratosphere to troposphere. Geophys Res Lett 4:363–365

Ishikawa Y, Murakami H, Sekine T et al (1995) Precipitation scavenging studies of radionuclides in air using cosmogenic Be-7. J Environ Radioact 26:19–36

Jungers MC, Bierman PR, Matmon A et al (2009) Tracing hillslope sediment production and transport with in situ and meteoric Be-10. J Geophys Res Earth Surf 114:16

Jweda J, Baskaran M, van Hees E et al (2008) Short-lived radionuclides (Be-7 and Pb-210) as tracers of particle

dynamics in a river system in southeast Michigan. Limnol Oceanogr 53:1934–1944
Kadko D (2000) Modeling the evolution of the Arctic mixed layer during the fall 1997 Surface Heat Budget of the Arctic Ocean (SHEBA) project using measurements of Be-7. J Geophys Res Oceans 105:3369–3378
Kadko D, Olson D (1996) Beryllium-7 as a tracer of surface water subduction and mixed-layer history. Deep Sea Res Part I Oceanogr Res Pap 43:89–116
Kadko D, Swart P (2004) The source of the high heat and freshwater content of the upper ocean at the SHEBA site in the Beaufort Sea in 1997. J Geophys Res Oceans 109:10
Kaste JM (1999) Dynamics of cosmogenic and bedrock-derived beryllium nuclides in forested ecosystems in Maine, USA. MSc Thesis, University of Maine
Kaste JM, Norton SA, Hess CT (2002) Environmental chemistry of beryllium-7. In: Grew E (ed) Beryllium: mineralogy, petrology, and geochemistry. Mineralogical Society of America, Washington
Kaste JM, Heimsath AM, Bostick BC (2007) Short-term soil mixing quantified with fallout radionuclides. Geology 35: 243–246
Kim SH, Hong GH, Baskaran M, Park KM, Chung CS, Kim KH (1998) Wet removal of atmospheric ^{7}Be and ^{210}Pb at the Korean Yellow Sea Coast. The Yellow Sea 4:58–68
Kiss JJ, De Jong E, Martz LW (1988) The distribution of fallout Cs-137 in Southern Saskatchewan, Canada. J Environ Qual 17:445–452
Knies DL, Elmore D, Sharma P et al (1994) Be-7, Be-10, and Cl-36 in precipitation. Nucl Instrum Meth Phys Res 92:340–344
Koch DM, Mann ME (1996) Spatial and temporal variability of Be-7 surface concentrations. Tellus Ser B Chem Phys Meteorol 48:387–396
Krishnaswami S, Benninger LK, Aller RC et al (1980) Atmospherically-derived radionuclides as tracers of sediment mixing and accumulation in near-shore marine and lake-sediments – evidence from Be-7, Pb-210, and Pu-239, Pu-240. Earth Planet Sci Lett 47:307–318
Krishnaswami S, Mangini A, Thomas JH et al (1982) Be-10 and Th isotopes in manganese nodules and adjacent sediments – nodule growth histories and nuclide behavior. Earth Planet Sci Lett 59:217–234
Ku TL, Kusakabe M, Nelson DE et al (1982) Constancy of oceanic deposition of Be-10 as recorded in manganese crusts. Nature 299:240–242
Ku TL, Kusakabe M, Measures CI et al (1990) Beryllium isotope distribution in the Western North-Atlantic – a comparison to the Pacific. Deep Sea Res Part I 37:795–808
Kusakabe M, Ku TL (1984) Incorporation of Be isotopes and other trace-metals into marine ferromanganese deposits. Geochim Cosmochim Acta 48:2187–2193
Kusakabe M, Ku TL, Vogel J et al (1982) Be-10 profiles in seawater. Nature 299:712–714
Kusakabe M, Ku TL, Southon JR et al (1987) Distribution of Be-10 and Be-9 in the Pacific Ocean. Earth Planet Sci Lett 82:231–240
Kusakabe M, Ku TL, Southon JR et al (1990) Beryllium isotopes in the ocean. Geochem J 24:263–272
Kusakabe M, Ku TL, Southon JR et al (1991) Be isotopes in river estuaries and their oceanic budgets. Earth Planet Sci Lett 102:265–276
Lal D (2007) Recycling of cosmogenic nuclides after their removal from the atmosphere; special case of appreciable transport of Be-10 to polar regions by aeolian dust. Earth Planet Sci Lett 264:177–187
Lal D (2011) Using cosmogenic radionuclides for the determination of effective surface exposure age and time-averaged erosion rates. In: Baskaran M (ed) Handbook of environmental isotope geochemistry. Springer, Heidelberg
Lal D, Baskaran M (2011) Applications of cosmogenic-isotopes as atmospheric tracers. In: Baskaran M (ed) Handbook of environmental isotope geochemistry. Springer, Heidelberg
Lal D, Malhotra PK, Peters B (1958) On the production of radioisotopes in the atmosphere by comic radiation and their application to meteorology. J Atmos Terr Phys 12:306–328
Lal D, Nijampurkar VN, Rajagopalan G, Somayajulu BLK (1979) Annual fallout of Si-32, Pb-210, Na-22, S-35 and Be-7 in rains in India. Proc Indian Natl Sci Acad 88:29–40
Lal D, Rama T, Zutshi PK (1960) Radioisotopes P-32, Be-7, and S-35 in the atmosphere. J Geophys Res 65:669–674
Lal D, Barg E, Pavich M (1991) Development of cosmogenic nuclear methods for the study of soil-erosion and formation rates. Curr Sci 61:636–640
Lao Y, Anderson RF, Broecker WS et al (1992a) Transport and burial rates of Be-10 and Pa-231 in the Pacific-Ocean during the Holocene period. Earth Planet Sci Lett 113:173–189
Lao Y, Anderson RF, Broecker WS et al (1992b) Increased production of cosmogenic Be-10 during the last glacial maximum. Nature 357:576–578
Larsen IL, Cutshall NH (1981) Direct determination of ^{7}Be in sediments. Earth Planet Sci Lett 54:379–384
Lee T, Barg E, Lal D (1991) Studies of vertical mixing in the southern California Bight with cosmogenic radionuclides P-32 and Be-7. Limnol Oceanogr 36:1044–1053
Leya I, Lange HJ, Neumann S et al (2000) The production of cosmogenic nuclides in stony meteoroids by galactic cosmic-ray particles. Meteor Planet Sci 35:259–286
Luo SD, Ku TL (2004a) On the importance of opal, carbonate, and lithogenic clays in scavenging and fractionating ^{230}Th, ^{231}Pa and ^{10}Be in the ocean. Earth Planet Sci Lett 220:201–211
Luo SD, Ku TL (2004b) Reply to comment on "On the importance of opal, carbonate, and lithogenic clays in scavenging and fractionating ^{230}Th, ^{231}Pa and ^{10}Be in the ocean". Earth Planet Sci Lett 220:223–229
Magilligan FJ, Nislow KH, Graber BE (2003) Scale-independent assessment of discharge reduction and riparian disconnectivity following flow regulation by dams. Geology 31:569–572
Mangini A, Segl M, Bonani G et al (1984) Mass spectrometric Be-10 dating of deep-sea sediments applying the Zurich tandem accelerator. Nucl Instrum Meth Phys Res Sect B Beam Interact Mater Atoms 5:353–358
Mangini A, Segl M, Kudrass H et al (1986) Diffusion and supply rates of Be-10 and Th-230 radioisotopes in 2 manganese encrustations from the South China Sea. Geochim Cosmochim Acta 50:149–156
Masarik J, Beer J (1999) Simulation of particle fluxes and cosmogenic nuclide production in the Earth's atmosphere. J Geophys Res Atmos 104:12099–12111
Masarik J, Beer J (2009) An updated simulation of particle fluxes and cosmogenic nuclide production in the Earth's atmosphere. J Geophys Res Atmos 114:9

Masque P, Cochran JK, Hirschberg DJ et al (2007) Radionuclides in Arctic sea ice: tracers of sources, fates and ice transit time scales. Deep Sea Res Part I 54:1289–1310

Matisoff G, Whiting PJ (2011) Measuring soil erosion rates using natural (^{7}Be, ^{210}Pb) and anthropogenic (^{137}Cs, ^{239,240}Pu) radionuclides. In: Baskaran M (ed) Handbook of environmental isotope geochemistry. Springer, Heidelberg

Matisoff G, Wilson CG, Whiting PJ (2005) The Be-7/Pb-210 (xs) ratio as an indicator of suspended sediment age or fraction new sediment in suspension. Earth Surf Process Landforms 30:1191–1201

McHargue LR, Damon PE (1991) The global beryllium 10 cycle. Rev Geophys 29:141–158

McKean JA, Dietrich WE, Finkel RC et al (1993) Quantification of soil production and downslope creep rates from cosmogenic Be-10 accumulations on a hillslope profile. Geology 21:343–346

McNeary D, Baskaran M (2003) Depositional characteristics of Be-7 and Pb-210 in southeastern Michigan. J Geophys Res Atmos 108:15

Measures CI, Ku TL, Luo S et al (1996) The distribution of Be-10 and Be-9 in the South Atlantic. Deep Sea Res Part I Oceanogr Res Pap 43:987–1009

Merrill JR, Lyden EFX, Honda M et al (1960) The sedimentary geochemistry of the beryllium isotopes. Geochim Cosmochim Acta 18:108–129

Monaghan MC, Krishnaswami S, Thomas JH (1983) Be-10 concentrations and the long-term fate of particle-reactive nuclides in 5 soil profiles from California. Earth Planet Sci Lett 65:51–60

Monaghan MC, Krishnaswami S, Turekian K (1986) The global-average production rate of ^{10}Be. Earth Planet Sci Lett 76:279–287

Monaghan MC, McKean J, Dietrich W et al (1992) Be-10 chronometry of bedrock-to-soil conversion rates. Earth Planet Sci Lett 111:483–492

Moore WS, Liu TZ, Broecker WS et al (2001) Factors influencing Be-7 accumulation on rock varnish. Geophys Res Lett 28:4475–4478

Morel J, Sepman S, Rasko M et al (2004) Precise determination of photon emission probabilities for main X- and gamma-rays of Ra-226 in equilibrium with daughters. Appl Radiat Isot 60:341–346

Murray AS, Marten R, Johnston A et al (1987) Analysis for naturally-occurring radionuclides at environmental concentrations by gamma spectrometry. J Radioanal Nucl Chem Artic 115:263–288

Nagai H, Tada W, Matsumura H et al (2004) Measurement of Be-7 at MALT. Nucl Instrum Meth Phys Res Sect B Beam Interact Mater Atoms 223:237–241

Nishiizumi K, Finkel RC, Klein J et al (1996) Cosmogenic production of Be-7 and Be-10 in water targets. J Geophys Res Solid Earth 101:22225–22232

Nishiizumi K, Imamura M, Caffee MW et al (2007) Absolute calibration of Be-10 AMS standards. Nucl Instrum Meth Phys Res Sect B Beam Interact Mater Atoms 258:403–413

Nurnberg D, Wollenburg I, Dethleff D et al (1994) Sediments in arctic sea ice-implications for entrainment, transport, and release. Mar Geol 119:185–214

Nyffeler UP, Li YH, Santschi PH (1984) A kinetic approach to describe trace-element distribution between particles and solution in natural aquatic systems. Geochim Cosmochim Acta 48:1513–1522

Olsen CR, Larsen IL, Lowry PD et al (1985) Atmospheric fluxes and marsh soil inventories of ^{7}Be and ^{210}Pb. J Geophys Res 90:10487–10495

Olsen CR, Larsen IL, Lowry PD et al (1986) Geochemistry and deposition of ^{7}Be in river-estuarine and coastal waters. J Geophys Res 91:896–908

Papastefanou C, Ioannidou A (1991) Depositional fluxes and other physical characteristics of atmospheric beryllium-7 in the temperate zones (40-degrees N) with a dry (precipitation-free) climate. Atmos Environ A Gen Topics 25:2335–2343

Pavich MJ, Brown L, Klein J et al (1984) Be-10 accumulation in a soil chronosequence. Earth Planet Sci Lett 68:198–204

Peirson DA (1963) ^{7}Be in air and rain. J Geophys Res 68:3831–3832

Pavich MJ, Brown L, Valettesilver N et al (1985) ^{10}Be analysis of a quaternary weathering profile in the Virginia Piedmont. Geology 13:39–41

Pavich M, Brown L, Harden JW et al (1986) ^{10}Be distribution in soils from Merced river terraces, California. Geology 50:1727–1735

Preiss N, Melieres MA, Pourchet M (1996) A compilation of data on lead 210 concentration in surface air and fluxes at the air-surface and water-sediment interfaces. J Geophys Res Atmos 101:28847–28862

Raisbeck GM, Yiou F (1988) Measurement of Be-7 by accelerator mass-spectrometry. Earth Planet Sci Lett 89:103–108

Raisbeck GM, Yiou F, Fruneau M et al (1978a) Be-10 mass spectrometry with a cyclotron. Science 202:215–217

Raisbeck GM, Yiou F, Fruneau M et al (1978b) Measurement of Be-10 in 1,000 year-old and 5,000 year old antarctic ice. Nature 275:731–733

Raisbeck GM, Yiou F, Fruneau M et al (1980) ^{10}Be concentration and residence time in the deep ocean. Earth Planet Sci Lett 51:275–278

Reimnitz E, Marincovich L, McCormick M et al (1992) Suspension freezing of bottom sediment and biota in the northwest passage and implications for arctic-ocean sedimentation. Can J Earth Sci 29:693–703

Robbins JA, Eadie BJ (1991) Seasonal cycling of trace-elements Cs-137, Be-7, and Pu-239+240 in Lake Michigan. J Geophys Res Oceans 96:17081–17104

Russell IJ, Choquette CE, Fang SL et al (1981) Forest vegetation as a sink for atmospheric particulates – quantitative studies in rain and dry deposition. J Geophys Res 86:5247–5363

Salant NL, Renshaw CE, Magilligan FJ et al (2007) The use of short-lived radionuclides to quantify transitional bed material transport in a regulated river. Earth Surf Process Landforms 32:509–524

Salisbury RT, Cartwright J (2005) Cosmogenic Be-7 deposition in North Wales: Be-7 concentrations in sheep faeces in relation to altitude and precipitation. J Environ Radioact 78:353–361

Sauve S, Hendershot W, Allen HE (2000a) Solid-solution partitioning of metals in contaminated soils: dependence on pH, total metal burden, and organic matter. Environ Sci Technol 34:1125–1131

Sauve S, Martinez CE, McBride M et al (2000b) Adsorption of free lead (Pb2+) by pedogenic oxides, ferrihydrite, and leaf compost. Soil Sci Soc Am J 64:595–599

Schuler C, Wieland E, Santschi PH et al (1991) A multitracer study of radionuclides in Lake Zurich, Switzerland. 1. Comparison of atmospheric and sedimentary fluxes of Be-7, Be-10, Pb-210, Po-210, and Cs-137. J Geophys Res Oceans 96:17051–17065

Schuller P, Iroume A, Walling DE et al (2006) Use of beryllium-7 to document soil redistribution following forest harvest operations. J Environ Qual 35:1756–1763

Segl M, Mangini A, Bonani G et al (1984a) Be-10 dating of the inner structure of Mn-encrustations applying the Zurich tandem accelerator. Nucl Instrum Meth Phys Res Sect B Beam Interact Mater Atoms 5:359–364

Segl M, Mangini A, Bonani G et al (1984b) Be-10 dating of a manganese crust from central North Pacific and implications for ocean paleocirculation. Nature 309:540–543

Segl M, Magini A, Beer J et al (1987) ^{10}Be in the Atlantic Ocean, a transect at 25 deg N. Nucl Instr Meth Phys Res B29:332–334

Sharma P, Somayajulu BLK (1982) Be-10 dating of large manganese nodules from world oceans. Earth Planet Sci Lett 59:235–244

Sharma P, Mahannah R, Moore WS et al (1987) Transport of Be-10 and Be-9 in the ocean. Earth Planet Sci Lett 86:69–76

Sheets RW, Lawrence AE (1999) Temporal dynamics of airborne lead-210 in Missouri (USA): implications for geochronological methods. Environ Geol 38:343–348

Silker WB (1972) Horizontal and vertical distributions of radionuclides in North Pacific ocean. J Geophys Res 77:1061

Silker WB, Robertson DE, Rieck HG et al (1968) Beryllium-7 in ocean water. Science 161:879–880

Simon SL, Bouville A, Beck HL (2004) The geographic distribution of radionuclide deposition across the continental US from atmospheric nuclear testing. J Environ Radioact 74: 91–105

Somayajulu BLK (1967) Beryllium-10 in a manganese nodule. Science 156:1219

Sommerfield CK, Nittrouer CA, Alexander CR (1999) Be-7 as a tracer of flood sedimentation on the northern California continental margin. Cont Shelf Res 19:335–361

Steinmann P, Billen T, Loizeau JI et al (1999) Beryllium-7 as a tracer to study mechanisms and rates of metal scavenging from lake surface waters. Geochim Cosmochim Acta 63:1621–1633

Svendsen KM, Renshaw CE, Magilligan FJ et al (2009) Flow and sediment regimes at tributary junctions on a -regulated river: impact on sediment residence time and benthic macroinvertebrate communities. Hydrol Process 23: 284–296

Takahashi Y, Minai Y, Ambe S et al (1999) Comparison of adsorption behavior of multiple inorganic ions on kaolinite and silica in the presence of humic acid using the multitracer technique. Geochim Cosmochim Acta 63:815–836

Tanaka S, Inoue T, Huang ZY (1982) Be-10 and Be-10/Be-9 in near Antarctica sediment cores. Geochem J 16:321–325

Todd JF, Wong GTF, Olsen CR et al (1989) Atmospheric depositional characteristics of beryllium-7 and lead-210 along the southeastern Virginia coast. J Geophys Res Atmos 94:11106–11116

Trimble SM, Baskaran M, Porcelli D (2004) Scavenging of thorium isotopes in the Canada basin of the Arctic Ocean. Earth Planet Sci Lett 222:915–932

Tsai H, Maejima Y, Hseu ZY (2008) Meteoric Be-10 dating of highly weathered soils from fluvial terraces in Taiwan. Quat Int 188:185–196

Turekian KK, Cochran JK, Krishnaswami S et al (1979) Measurement of Be-10 in manganese nodules using a tandem vandergraaff accelerator. Geophys Res Lett 6:417–420

Turekian KK, Benninger LK, Dion EP (1983) Be-7 and Pb-210 total deposition fluxes at New Haven, Connecticut and at Bermuda. J Geophys Res 88:5411–5415

Vesely J, Benes P, Sevcik K (1989) Occurrence and speciation of beryllium in acidified freshwaters. Water Res 23:711–717

Vogler S, Jung M, Mangini A (1996) Scavenging of Th-234 and Be-7 in Lake Constance. Limnol Oceanogr 41:1384–1393

von Blanckenburg F, O'Nions RK, Belshaw NS et al (1996) Global distribution of beryllium isotopes in deep ocean water as derived from Fe-Mn crusts. Earth Planet Sci Lett 141:213–226

Vonmoos M, Beer J, Muscheler R (2006) Large variations in Holocene solar activity: constraints from Be-10 in the Greenland Ice Core Project ice core. J Geophys Res Space Phys 111:A10105

Wallbrink PJ, Murray AS (1994) Fallout of Be-7 in South Eastern Australia. J Environ Radioact 25:213–228

Wallbrink PJ, Murray AS (1996) Distribution and variability of Be-7 in soils under different surface cover conditions and its potential for describing soil redistribution processes. Water Resour Res 32:467–476

Wallbrink PJ, Murray AS, Olley JM (1999) Relating suspended sediment to its original soil depth using fallout radionuclides. Soil Sci Soc Am J 63:369–378

Walling DE, He Q, Blake W (1999) Use of Be-7 and Cs-137 measurements to document short- and medium-term rates of water-induced soil erosion on agricultural land. Water Resour Res 35:3865–3874

Walling DE, Schuller P, Zhang Y et al (2009) Extending the timescale for using beryllium 7 measurements to document soil redistribution by erosion. Water Resour Res 45:13

Walton A, Fried RE (1962) The deposition of ^{7}Be and ^{32}P in precipitation at north temperate latitudes. J Geophys Res 67:5335–5340

Whiting PJ, Bonniwell EC, Matisoff G (2001) Depth and areal extent of sheet and rill erosion based on radionuclides in soils and suspended sediment. Geology 29:1131–1134

Whiting PJ, Matisoff G, Fornes W (2005) Suspended sediment sources and transport distances in the Yellowstone River basin. Geol Soc Am Bull 117:515–529

Willenbring JK, von Blanckenburg F (2010a) Meteoric cosmogenic Beryllium-10 adsorbed to river sediment and soil: applications for earth-surface dynamics. Earth Sci Rev 98: 105–122

Willenbring JK, von Blanckenburg F (2010b) Long-term stability of global erosion rates and weathering during late-Cenozoic cooling. Nature 465:211–214

Wilson CG, Matisoff G, Whiting PJ (2003) Short-term erosion rates from a Be-7 inventory balance. Earth Surf Process Landforms 28:967–977

You CF, Lee T, Li YH (1989) The partitioning of Be between soil and water. Chem Geol 77:105–118

Zhu J, Olsen CR (2009) Beryllium-7 atmospheric deposition and sediment inventories in the Neponset River estuary, Massachusetts, USA. J Environ Radioact 100:192–197